AFML-TR-71-31

TECHNOLOGY DEVELOPMENT FOR TRANSITION METAL-RARE EARTH HIGH-PERFORMANCE MAGNETIC MATERIALS

Contract No. F33615-70-C-1626
Sponsored by the Advanced Research Projects Agency
ARPA Order No. 1617, Program Code No. OD10
Contract effective date: 30 June 1970. Expiration date: 30 June 1973
Amount of contract: $579,000.

Submitted to:

Air Force Materials Laboratory, AFSC, USAF
Project Engineer: J.C. Olson, LPE, Tel. (513) 255-4474

By:

J.J. Becker, Principal Investigator, Tel. (518) 346-8771, Ext. 6114
GENERAL ELECTRIC COMPANY
CORPORATE RESEARCH AND DEVELOPMENT
P.O. Box 8
SCHENECTADY, NEW YORK 12301

The views and conclusions contained in this document are those of the authors and should not be interpreted as necessarily representing the official policies, either expressed or implied, of the Advanced Research Projects Agency or the U.S. Government.

45

DISCLAIMER NOTICE

THIS DOCUMENT IS BEST QUALITY PRACTICABLE. THE COPY FURNISHED TO DTIC CONTAINED A SIGNIFICANT NUMBER OF PAGES WHICH DO NOT REPRODUCE LEGIBLY.

NOTICE

When Government drawings, specifications, or other data are used for any purpose other than in connection with a definitely related Government procurement operation, the United States Government thereby incurs no responsibility nor any obligation whatsoever; and the fact that the government may have formulated, furnished, or in any way supplied the said drawings, specifications, or other data, is not to be regarded by implication or otherwise as in any manner licensing the holder or any other person or corporation, or conveying any rights or permission to manufacture, use, or sell any patented invention that may in any way be related thereto.

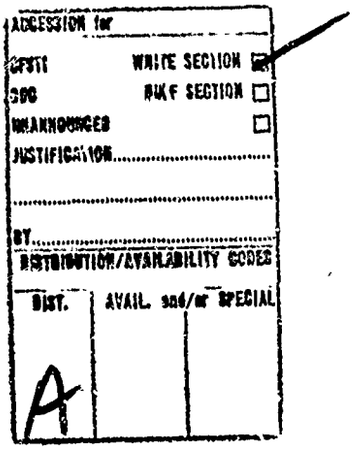

Copies of this report should not be returned unless return is required by security considerations, contractual obligations, or notice on a specific document.

UNCLASSIFIED

Security Classification

DOCUMENT CONTROL DATA - R & D

(Security classification of title, body of abstract and indexing annotation must be entered when the overall report is classified)

1 ORIGINATING ACTIVITY (Corporate author) General Electric Company Corporate Research and Development Schenectady, New York	2a. REPORT SECURITY CLASSIFICATION Unclassified 2b. GROUP

3 REPORT TITLE

TECHNOLOGY DEVELOPMENT FOR TRANSITION METAL-RARE EARTH HIGH-PERFORMANCE MAGNETIC MATERIALS

4. DESCRIPTIVE NOTES (Type of report and inclusive dates)

First Semi-Annual Interim Technical Report June 30, 1970 to December 31, 1970

5. AUTHOR(S) (First name, middle initial, last name)

Joseph J. Becker

6. REPORT DATE	7a. TOTAL NO OF PAGES	7b. NO OF REFS
April 1971	35	23

8a. CONTRACT OR GRANT NO.	9a. ORIGINATOR'S REPORT NUMBER(S)
F33615-70-C-1626 b. PROJECT NO ARPA Order No. 1617 c. Program Code No. OD10 d.	S-71-1047 9b. OTHER REPORT NO(S) (Any other numbers that may be assigned this report) AFML-TR-71-31

10. DISTRIBUTION STATEMENT This document has been approved for public release and sale; its distribution is unlimited.

11. SUPPLEMENTARY NOTES	12 SPONSORING MILITARY ACTIVITY
	Air Force Materials Laboratory (LPE) Wright-Patterson Air Force Base Ohio 45433

13. ABSTRACT Magnetization reversal discontinuities were studied in samples consisting of a few particles or a single particle. Experiments with successive polishing treatments indicate that individual defects are responsible for the observed magnetization behavior. A particle of Co_5Y showed a perfectly rectangular hysteresis loop and a maximum energy product of 27.6 mGOe. It has been found possible to analyze complex single-particle loops into linear combinations of elementary loops, as though the particles consisted of independent sub-particles. Metallographic studies of as-cast and annealed alloys of various compositions indicated that annealing has little effect on the observed phase distribution. Polarized light studies of finished magnets showed a greater tendency toward multidomain structures in magnets with lesser properties. A technique for analyzing the rare earth present in a compound in the reduced state indicated that this may be substantially less than the total rare earth present. Studies of Co-Nd-Sm and Co-Pr-Nd-Sm, aimed toward energy products of 25 mGOe or more, indicate that Nd and Pr combined are more effective than Nd alone in increasing the saturation, and that the variation of properties in these alloys is quite different from what it is in the Co-Pr-Sm alloys. An energy product of 20 mGOe has been attained in a Co-Pr-Nd-Sm alloy, although the optimum composition has not yet been reached.

DD FORM 1 NOV 65 1473

UNCLASSIFIED

Security Classification

14 KEY WORDS	LINK A		LINK B		LINK C	
	ROLE	WT	ROLE	WT	ROLE	WT
Magnetic Materials						
Permanent Magnets						
Cobalt-Rare Earth						
Magnetism						

TECHNOLOGY DEVELOPMENT FOR TRANSITION METAL-RARE EARTH HIGH-PERFORMANCE MAGNETIC MATERIALS

J.J. Becker

FOREWORD

This report describes work carried out in the Metallurgy and Ceramics Laboratory of the General Electric Research and Development Center, Schenectady, New York, under USAF Contract No. F33 615-70-C-1626, entitled "Technology Development for Transition Metal-Rare Earth High-Performance Magnetic Materials." This work is administered by the Air Force Materials Laboratory, Wright-Patterson AFB, Ohio, J. C. Olson Project Engineer.

This First Semi-Annual Interim Technical Report covers work conducted during the period 30 June - 31 December 1970. The principal participants in the research are J. J. Becker, J. D. Livingston, R. E. Cech, J. G. Smeggil, and D. L. Martin.

This technical report has been reviewed and is approved.

Charles E. Ehrenfried

CHARLES E. EHRENFRIED
Major, USAF
Chief, Electromagnetic Materials Branch
Materials Physics Division
Air Force Materials Laboratory

ABSTRACT

Magnetization reversal discontinuities were studied in samples consisting of a few particles or a single particle. Experiments with successive polishing treatments indicate that individual defects are responsible for the observed magnetization behavior. A particle of Co_5Y showed a perfectly rectangular hysteresis loop and a maximum energy product of 27.6 mGOe. It has been found possible to analyze complex single-particle loops into linear combinations of elementary loops, as though the particles consisted of independent sub-particles. Metallographic studies of as-cast and annealed alloys of various compositions indicated that annealing has little effect on the observed phase distribution. Polarized light studies of finished magnets showed a greater tendency toward multidomain structures in magnets with lesser properties. A technique for analyzing the rare earth present in a compound in the reduced state indicated that this may be substantially less than the total rare earth present. Studies of Co-Nd-Sm and Co-Pr-Nd-Sm, aimed toward energy products of 25 mGOe or more, indicate that Nd and Pr combined are more effective than Nd alone in increasing the saturation, and that the variation of properties in these alloys is quite different from what it is in the Co-Pr-Sm alloys. An energy product of 20 mGOe has been attained in a Co-Pr-Nd-Sm alloy, although the optimum composition has not yet been reached.

TABLE OF CONTENTS

LIST OF ILLUSTRATIONS

List of Illustrations (contd)

I. INTRODUCTION

This is the first semi-annual interim technical report for Contract No. F33615-70-C-1626. The objective of this work, as set forth in Exhibit A of the contract, is to develop the technology of high-performance transition metal-rare earth magnets for critical applications. High performance permanent magnets are defined in this context as those having remanences greater than ten thousand gauss and permeabilities of very nearly unity throughout the second and into the third quadrants of their hysteresis loop. Such technology is to be developed through studies of the origin of the intrinsic coercive force in high-anisotropy materials, development of information on phase equilibria in these systems, and identification and investigation of new materials. The progress that has been made during the period covered by this report is described below under these three major headings.

II. FUNDAMENTAL STUDIES OF THE ORIGIN OF THE COERCIVE FORCE IN HIGH-ANISOTROPY MATERIALS

1. Magnetization Studies in Single Particles (J. J. Becker)

It has previously been observed[1, 2, 3, 4] that individual particles of Co_5Sm can show sudden discontinuities in M as a function of H as the particle traverses a hysteresis loop. The values of H at which these jumps occur are quite discrete and reproducible for a given particle[1, 2]. This behavior suggests very strongly that the magnetic properties of such particles, and of bulk permanent magnets made from this material, are determined by imperfections whose function is to act as nuclei or pinning sites for domain boundaries. Since the observed nucleating fields or coercive forces are at most a few percent of $2K/M_S$, large-scale magnetization rotation must be negligible, with magnetization rotation occurring only in the interior of a domain boundary. Imperfections thus become important by acting as nuclei for such local rotations. It seems clear that an understanding of the factors influencing the occurrence of magnetization jumps is the key to the solution of the major unsolved problems in the cobalt-rare-earths, including not only the discrepancy between achievable properties, good as they are, and what appears to be theoretically possible, but also the closely related problem of the difference between the magnetic behavio Co_5Sm and that of other compounds that appear to be practically identic from a structural and chemical point of view.

These experiments are made possible by the use of the vibrating-sample magnetometer. During the period of the present report, the instrument that has been in use for some time[5] has been considerably improved. The vibrating head has been replaced by one mounted on a precision three-dimensional mechanical positioning unit, a rotating sample holder has been constructed, and the electronic system has been updated. Complete hysteresis loops of particles consisting of a few micrograms of material can be drawn

on an x-y recorder, with a relative accuracy in M of one percent or so. Zijlstra[6] has succeeded in measuring considerably smaller particles by a point-by-point method utilizing a vibrating reed.

A pair of pole pieces has been constructed on the principle that the maximum field attainable in a magnetic circuit depends not on its size but on its relative dimensions. The samples used in the vibrating-sample magnetometer are so small that the high fields necessary for their investigation can be attained in a small volume using only the 5-inch magnet on which the vibrating-sample magnetometer is mounted. The working space is a gap of 0.060 inch with a diameter of 0.100 inch. The field is about 44,000 oersteds.

Preliminary experiments

In one experiment, a sample was prepared that consisted of three particles of Co_5Sm. These were each about 100μ in average dimension. They had been prepared from a magnetically sieved[1, 2] powder prepared from a cast ingot that analyzed 66.8% Co (nominal Co_5Sm is 66.2). They had also been chemically polished[1, 2] in a solution consisting of 3 parts HNO_3, 1 part H_2SO_4, 1 part H_3PO_4, and 5 parts CH_3COOH by volume. They were mounted in paraffin in the tip of a small glass capillary tube, so that they were in contact with each other, and aligned in a field as the paraffin solidified. Hysteresis loops at various maximum magnetizing fields H_m were measured in a vibrating-sample magnetometer. Some of these loops are shown, superimposed, in Fig. 1. A number of interesting features appear. In 5 kOe, the hysteresis loop resulting from free wall motion can be seen. Its slope is determined by the sample shape and corresponds to an effective shape demagnetizing field of about 3000 Oe. As H_m is increased, very pronounced jumps appear, along with curved segments. At large H_m, the reversal takes place almost entirely by jumps. It seems clear that the curved segments, including the entire 5 kOe loop, are due to gradual wall motion, while the sudden jumps are caused by the nucleation or unpinning and abrupt motion of a wall. The curves drawn at different H_m often have segments that appear to be continuations of each other, and frequently have jumping field values in common. Often the absolute value of the field at which a jump occurs is the same for both senses of H, strongly suggesting that the domain configuration at that point is the same except with the directions of magnetization reversed. Individual loops can be highly unsymmetrical, as for example the 15 kOe loop. It is interesting to note that at high H_m the magnetization reversal may be complete in two jumps, even though three particles are present.

Experiments were then performed on single particles. Figure 2 shows some results for a sample consisting of a single particle of this same material that was originally approximately 100μ in each dimension. The field at which the jump occurred, H_n, is plotted vertically and the previous magnetizing field H_m is shown horizontally. The sign of H_n is such that a positive

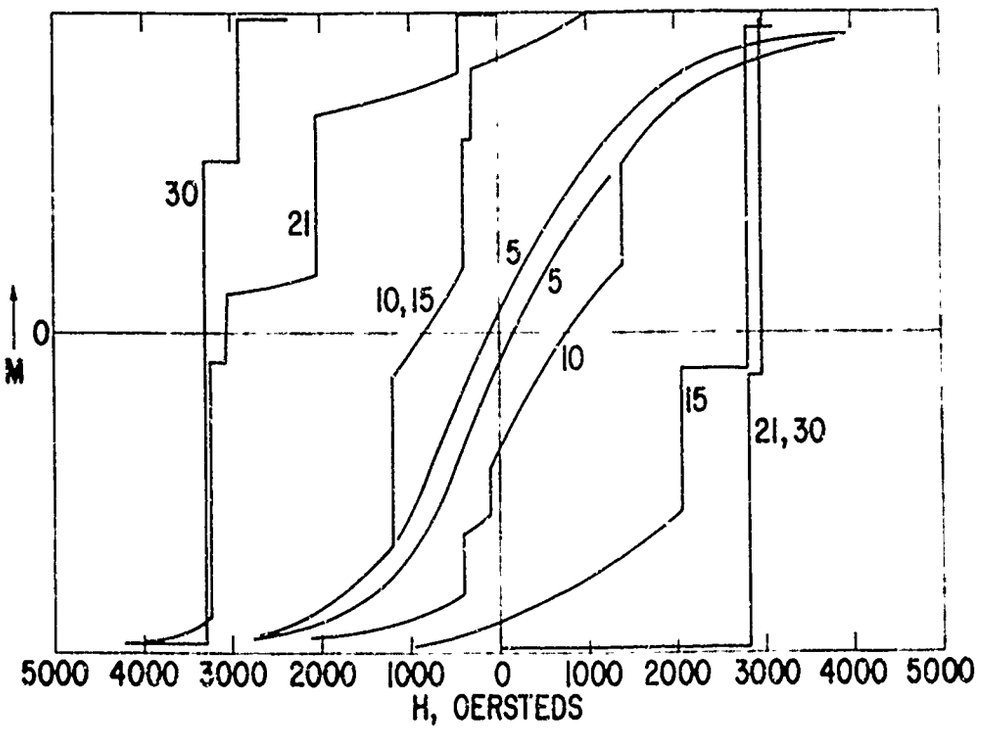

Fig. 1 Hysteresis loops of a sample consisting of three particles of Co_5Sm for various values of maximum magnetizing field H_m. Numbers next to loops are values of H_m in kOe.

value corresponds to the same direction as H_m and a negative value to the opposite direction. Of course, H_n, which is the applied field, always corresponds to a negative internal field. The trend that can be seen in Fig. 2 is that chemical polishing tends to produce jumps at less positive or more negative fields, that is, to remove the strongest nucleating sites. A strong site is here defined as one that produces a large local demagnetizing field and thus contributes to a low coercive force. Heating in air, in these preliminary experiments, seems to add new strong sites. Generally speaking, observed values of H_n seem to appear and disappear rather than being gradually modified by chemical treatment or aging, again suggesting that magnetization jumps are associated with discrete imperfections that are either present or entirely absent. The dependence of coercive force on H_m and on particle size is inherently discontinuous.

Remarkable behavior of Co_5Y particle

A single particle of stoichiometric Co_5Y was prepared and mounted as above. As ground, it showed mostly the wall-motion loop, with only two small jumps at +550 and -350 Oe, at all H_m from 5 to 30 kOe. This behavior

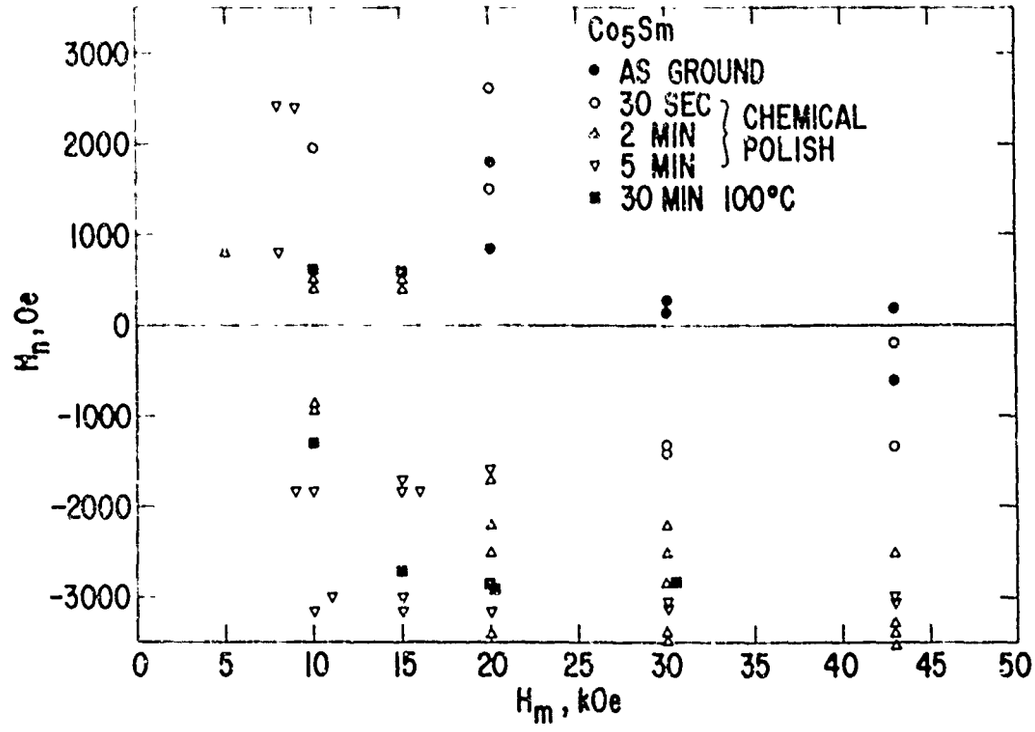

Fig. 2 Behavior of a single particle of Co_5Sm after various treatments. The applied field H_n at which magnetization jumps take place is shown as a function of the previously applied magnetizing field H_m.

persisted through successive treatments in the chemical polishing solution totaling 5 minutes. After two additional minutes, the behavior of the sample changed completely. By this time it had been reduced to about 40% of its original volume. The hysteresis loop, a photograph of which is shown in Fig. 3, became a perfect rectangle, with the magnetization reversing abruptly at 3800 Oe. Furthermore, this was true at all H_m down to 4100 Oe. It is remarkable that Co_5Y, which so far has not proven very tractable as a permanent-magnet material, shows such ideal behavior in single-particle form.

Most remarkable of all is the energy product of this particle. The perfect rectangularity of the hysteresis loop of this aligned particle means that the magnetization is equal to its saturation value. Then B_r is $4\pi M_s$, or 10,600 gauss. In a field of -3800 Oe, B would be 6800 gauss, for a maximum energy product of 25.8×10^6 gauss-Oe. If one corrects for the demagnetizing field of 800 Oe, measured from the free-wall hysteresis loop of this rather elongated particle, H_c is 4600 Oe and $(BH)_{max} = 27.6 \times 10^6$ gauss-Oe. This procedure can be justified on the basis that the reversal process does not depend inherently on the shape of the particle, in contrast to the

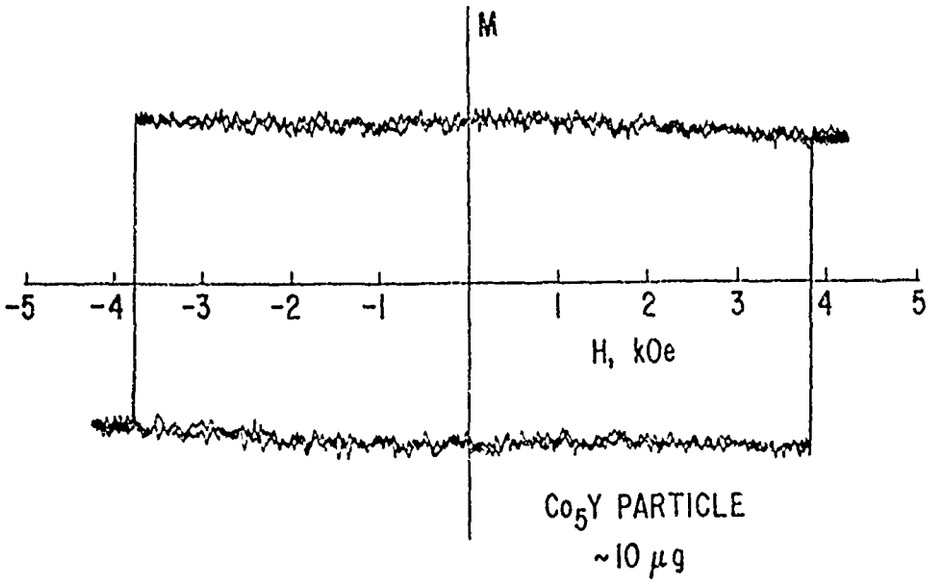

Fig. 3 Hysteresis loop of a single particle of Co_5Y. H_c = 3800 Oe, H_m = 4200 Oe. Loop traced twice in vibrating-sample magnetometer.

Stoner-Wohlfarth coherent-rotation mechanism. In either case, the energy product is believed to be the largest ever observed in any material at room temperature.

An attempt was made to measure H_n as a function of H_{ri} for small H_m. As with any truly square-loop material, it was somewhat difficult to get inside the major hysteresis loop. The results are shown in Fig. 4.

Analysis of single-particle hysteresis loops

Next, in view of the type of behavior shown in a general way in Fig. 1, more detailed studies of single particles were performed. These resulted in the discovery that the behavior of a typical particle could be analyzed as a superposition of elementary hysteresis loops.

For the purpose of this analysis, true single-particle behavior is defined as follows: In low magnetizing fields H_m the hysteresis loop is that corresponding to the motion of a wall already present. This loop will be narrow and in general somewhat curved. For a spherical sample, it can be linear, as in Fig. 5. The average field at which saturation is reached, H_d, is in this case $4\pi M_s/3$ and in general NM_s, where N is the demagnetizing factor of the particle, to the extent that its shape permits this sort of description. In general, in irregularly shaped samples, wall-motion loops are somewhat curved, as in Fig. 8a. The second feature of single-particle behavior is that

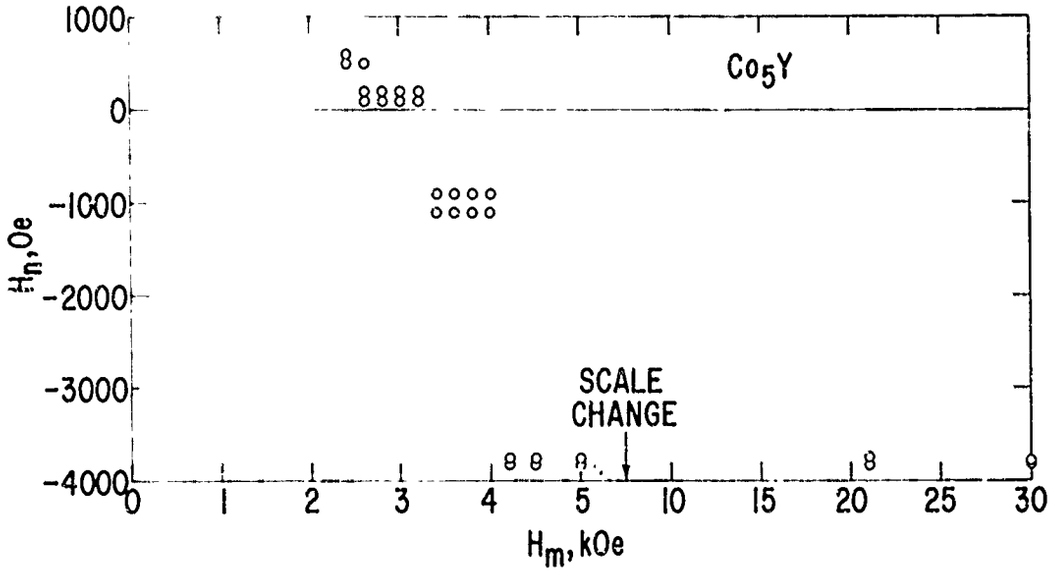

Fig. 4 Magnetization discontinuity field H_n as a function of previous magnetizing field H_m for a single particle of Co_5Y.

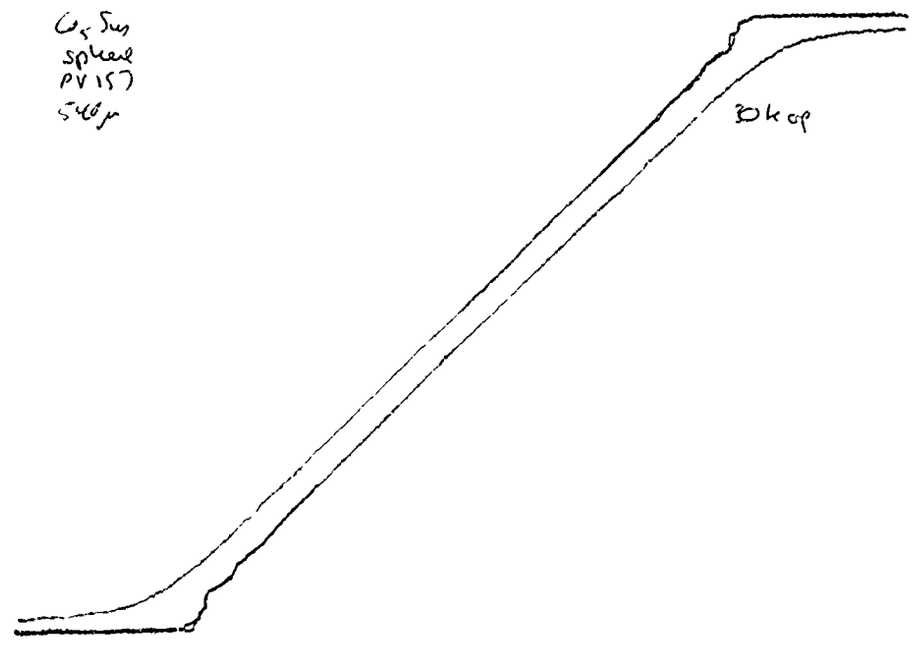

NOT REPRODUCIBLE

Fig. 5 Hysteresis loop of Co_5Sm sphere 540μ in diameter.

as H_m is increased, magnetization jumps appear at negative internal fields, that is, at applied fields less than H_d. These jumps appear at various discrete fields that correspond to some discrete nucleation process in the sample. Such jumps may be symmetrical, in which case the numerical value of the H_n corresponding to a certain H_m is the same for either direction of magnetization, or unsymmetrical, where the absolute value of H_n is different for $+H_m$ and $-H_m$. The symmetrical case presumably corresponds to the same nucleation site being active for either direction of magnetization, while in the unsymmetrical case a wall that nucleates at $+H_n$ is not completely driven out in $-H_m$ but a little of it remains to act as a nucleus at a different $-H_n$[7]. In any case, once nucleated, the wall moves in the field H_n until the magnetization reaches the value on the wall-motion loop, as in Fig. 6. At this point, the field on the wall is the wall-motion coercive force and further motion does not take place unless H changes. The wall would not completely reverse the particle unless H_n after a positive H_m were more negative than $-H_d$ (Fig. 6). This is an important point in what follows.

A measured symmetrical single-particle loop of the type described is shown in Fig. 7. Its correspondence with the behavior shown in Fig. 6 is evident.

Often what looks like a single particle will show more complicated behavior. For example, hysteresis loops in H_m of 5, 16, and 21 kOe for a particle of Co_5Sm about 50 microns in average diameter are reproduced in Fig. 8 a, b, c. This particle is actually much smaller than the one whose simpler behavior is shown in Fig. 7. The 16 and 21 kOe curves are, however,

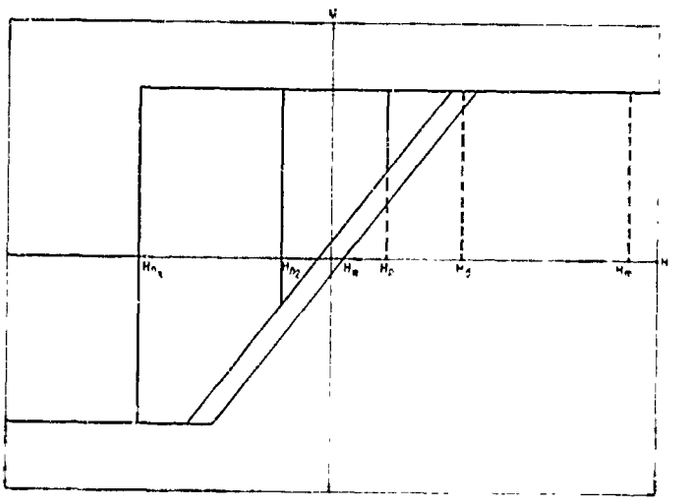

Fig. 6 Predicted behavior of single particle reversing by wall motion. H_m is the maximum magnetizing field, H_d the sample demagnetizing field, H_w the wall coercive force, and H_{n_1}, H_{n_2}, and H_{n_3} various nucleating fields.

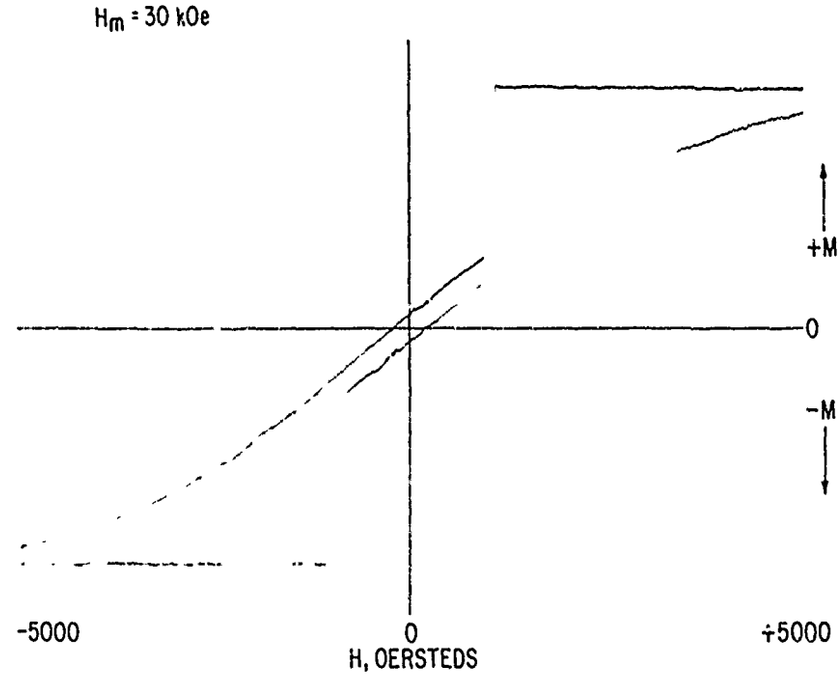

Fig. 7 Single-particle hysteresis loops in a Co_5Sm particle.

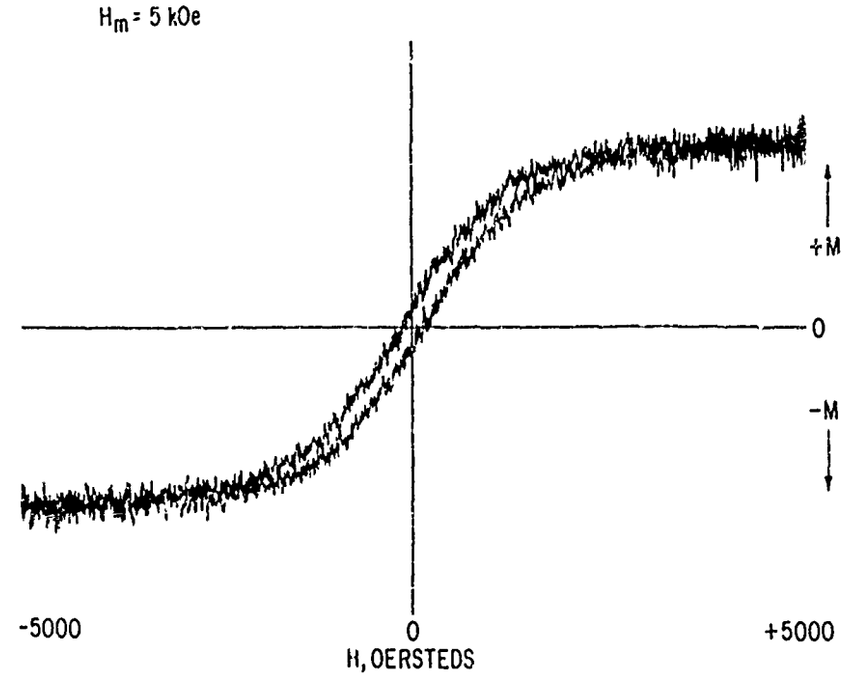

(a) H_m = 5 kOe.

Fig. 8 Hysteresis loops of a Co_5Sm particle.

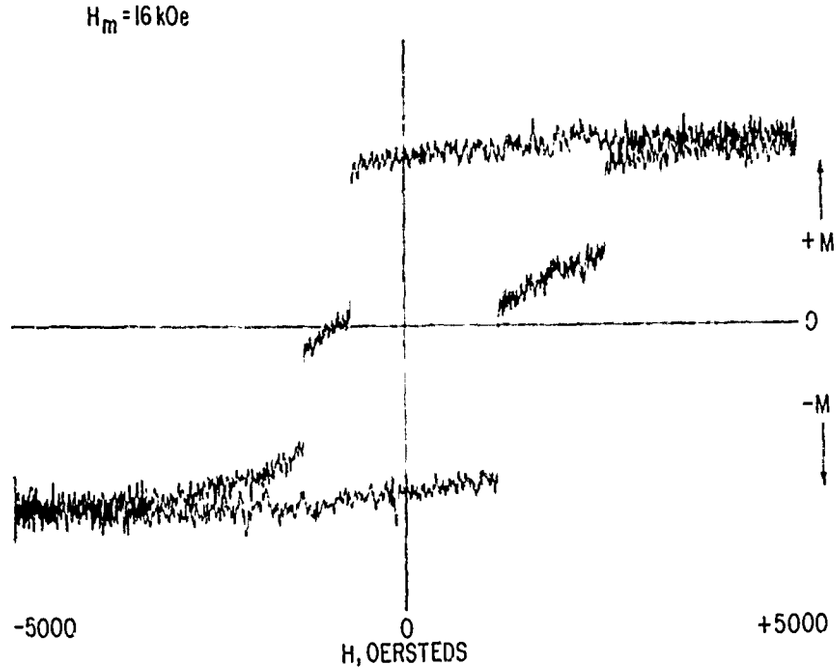

(b) H_m = 16 kOe.

Fig. 8 (continued).

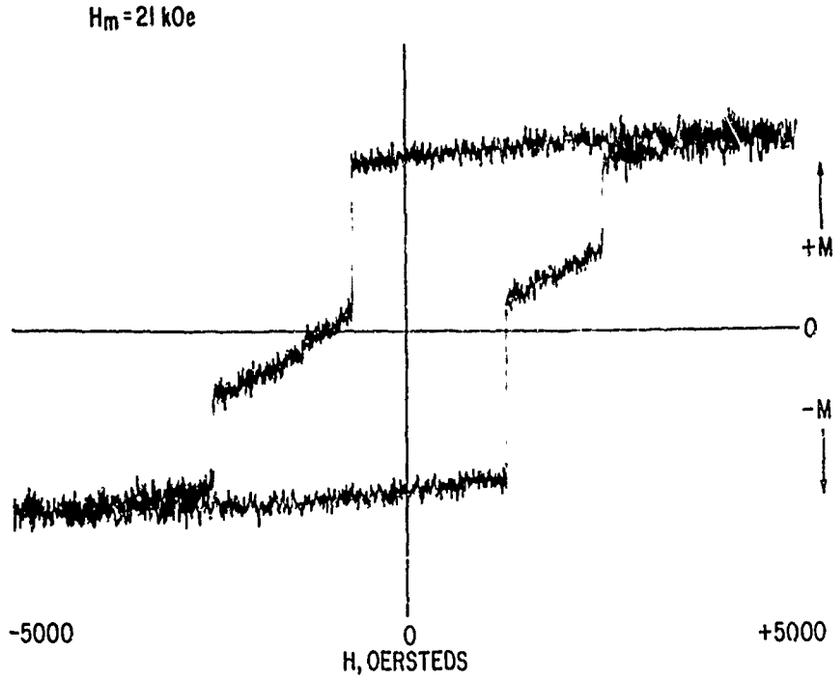

(c) H_m = 21 kOe.

Fig. 8 (continued).

more complicated. They are similar to the general type of behavior that has been observed in still smaller single particles by Zijlstra[4]. He discusses the behavior of his samples in terms of nucleation sites and pinning sites, which are taken to be two different entities. These have the rather specialized properties that pinning sites are located primarily near the surface and that aging in air has no effect on nucleation sites, but reduces the number of pinning sites without affecting their individual strengths. However, for the sample shown in Fig. 8, the description can be very much simplified. Each hysteresis loop can be constructed from the linear superposition of two "single-particle" loops, as defined above, just as though the sample really consisted of two entirely discrete single particles. The constituent loops are shown in Fig. 9a, c and 9b, d and their resultants in Fig. 9e and f. These are compared with the observed loops in Fig. 10. The magnetization scale in Fig. 9a, c and 9b, d is the same, and the value of saturation magnetization is simply proportional to the volume of material acting like an independent particle.

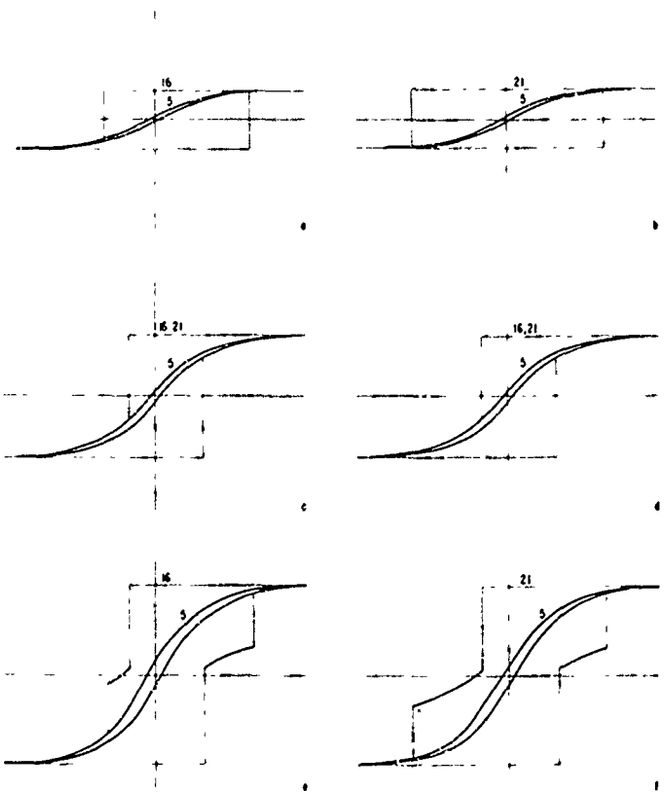

Fig. 9 Synthesis of complex hysteresis loops from single-particle loops. Numbers on loops are H_m in kOe. Fig. 9e is 9a + 9c, and 9f is 9b + 9d. Fig. 9a and 9b are one region of the particle in different H_m, 9c and 9d are another, and 9e and 9f are the entire particle, composed of these two regions.

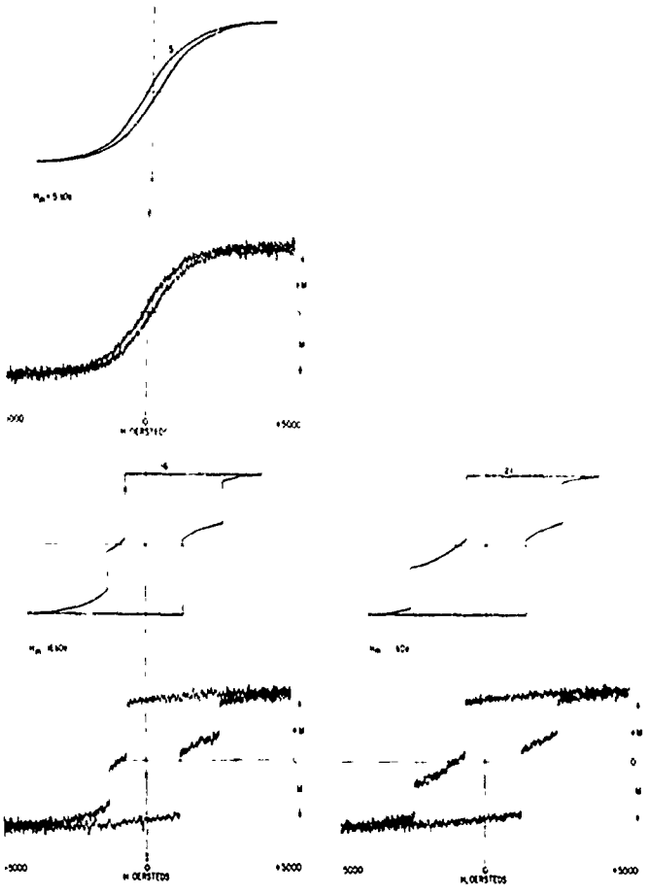

Fig. 10 Comparison of 5, 16, and 21 kOe loops from Fig. 9e and 9f with measured loops shown in Fig. 8.

On this model, the end of a magnetization jump has nothing whatever to do with pinning but occurs simply because the wall has arrived at the point where the field on it is no longer greater than the wall coercive force. The next jump results from another wall being nucleated elsewhere in the sample. Again this is in contrast to Zijlstra's view in which the entire branch of the hysteresis loop tends to be regarded as a record of the vicissitudes of a single wall as it is alternately pinned and freed.

This analysis raises the question of how it is that what looks under the microscope like a single particle can act as though it were two magnetically separate entities. The domain structure that results from a nucleation step may well be of some complexity, such as the labyrinth type of structure visible for example in one grain of Fig. 16. Kooy and Enz[8] found that nucleation corresponded to the appearance of this type of structure radiating from one spot in their single crystal barium ferrite samples. Particles that

reverse completely, and consequently do not show this structure statically, doubtless have it during a reversal. The labyrinth structure, originating at a nucleus, propagates because of its effectiveness in reducing magnetostatic energy. It can readily turn or branch as it propagates, and will probably do so rather than crossing a boundary, even of low energy. Thus, it may be that small particles that do not act like "single" particles contain low-angle boundaries. Indeed, all the grains in Fig. 16 are separated by low-angle boundaries, since the preferred orientation in this magnet is quite high. This may provide a clue to the question of how it is that a cobalt-samarium or barium ferrite magnet that is over 95% dense still has properties that so closely approximate those of the particles from which it is made.

2. Microscopy and Domain Structure of Alloys and Finished Magnets (J. D. Livingston)

Metallographic Studies

As-Cast. Pieces were broken from arc-cast ingots, polished, etched with 1% nital and 5% hydrol, and observed by standard optical microscopy. Ingots studied included: Co-Sm alloys containing 31.5, 33, 33.5, 34, 34.5, 35, 36, and 37 wt% Sm; Co-Pr alloys containing 32.4, 50, and 60 wt% Pr; and a Co-La alloy with 60 wt% La.

All as-cast Co-Sm alloys showed a two-phase structure. The second phase, appearing gray and presumed to be Co_7Sm_2, appeared in increasing volume fraction as Sm content increased. For 31.5 wt% Sm, the Co_7Sm_2 appeared only as small isolated regions occupying less than 5 percent of the sample. For 37 wt% Sm, the Co_7Sm_2 occupied approximately 40 percent of the sample (Fig. 11). Intermediate compositions had intermediate structures.

The Co-32.4 wt% Pr alloy showed only a small volume fraction of isolated particles of a second phase, presumably Pr-rich. Alloys containing 50 and 60 wt% Pr, and the alloy containing 60 wt% La, showed complex microstructures with at least three prominent phases.

Annealed. Pieces broken from various arc-cast ingots of Co-Sm alloys were annealed in vacuum 2 hours at 1100°C and subsequently subjected to metallographic examination. The gray second phase, identified earlier as Co_7Sm_2, was not present in the alloy containing 33 wt% Sm. Presumably this phase dissolved as a result of homogenization during the anneal. However, samples of 34, 35, 36, and 37 wt% Sm all contained substantial Co_7Sm_2 (e.g., Figs. 12 and 13), the volume fractions differing very little from those observed in the as-cast ingots.

Sintered Powder Magnets. Two sintered Co-Sm-Pr magnets of very different magnetic properties were sectioned transverse to the magnetization direction and examined to detect differences in microstructure. Magnet P-286

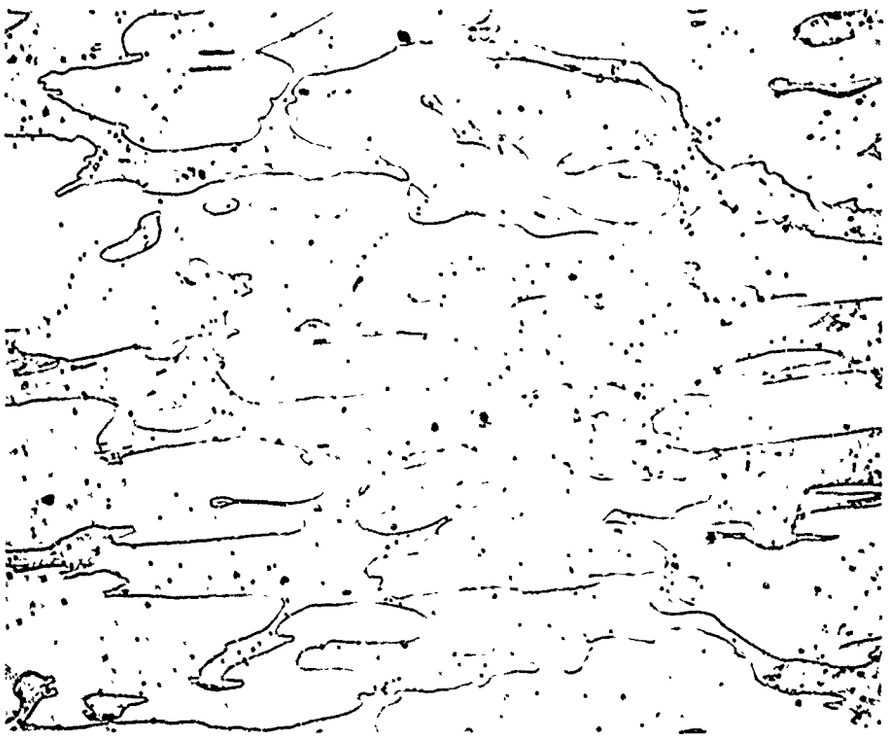

Fig. 11 63% Co + 37% Sm. As cast. Darker phase is Co_7Sm_2. 500X

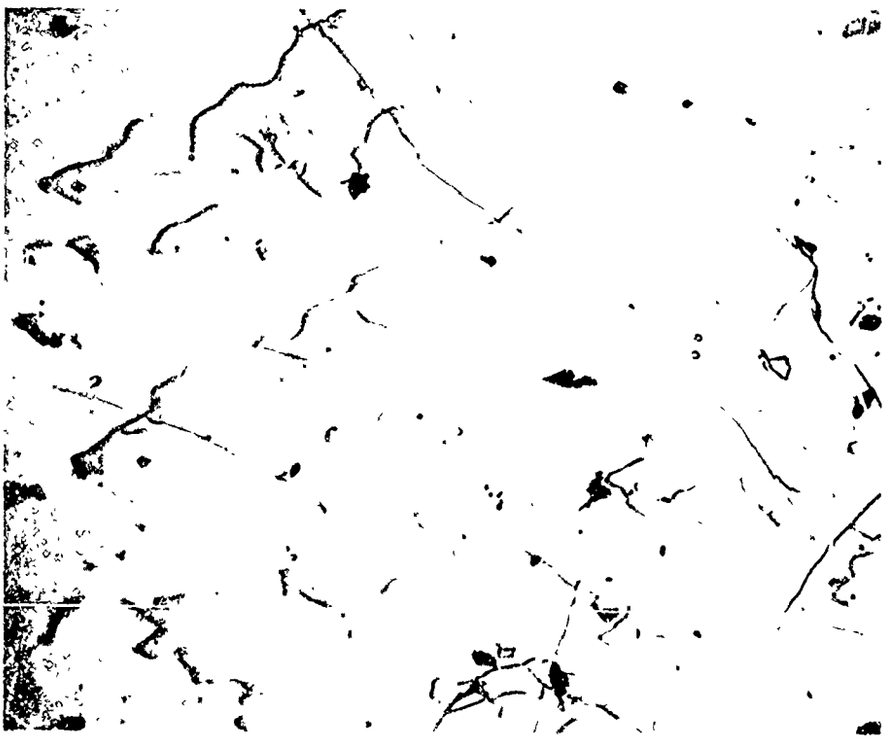

Fig. 12 66% Co + 34% Sm. Annealed 2 hours in vacuum at 1100°C. 500X

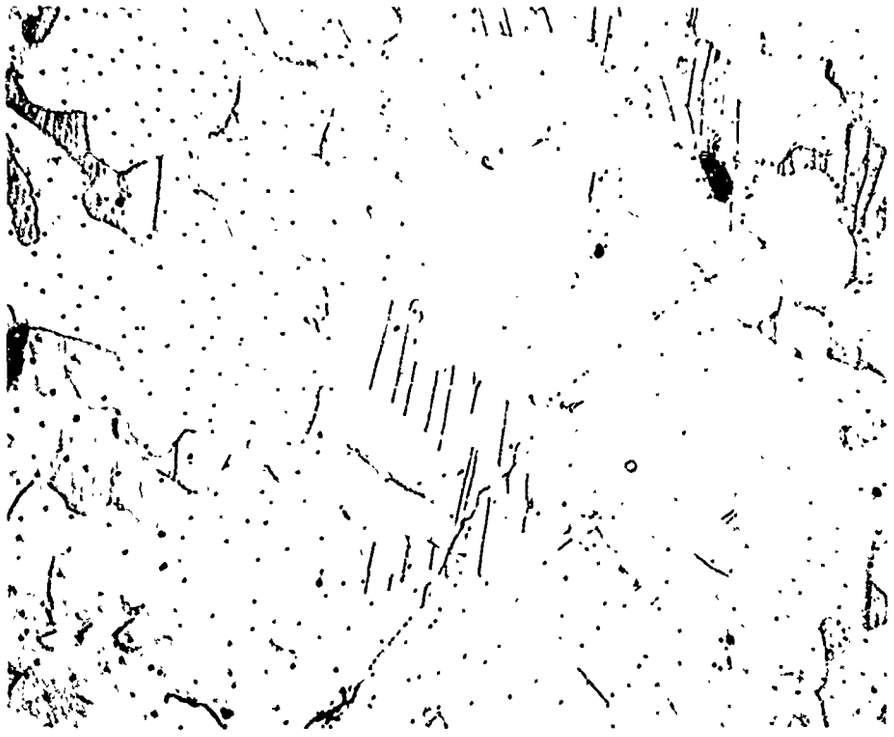

Fig. 13 64% Co + 36% Sm. Annealed 2 hours in vacuum at 1100°C. 500X

had an intrinsic coercive force of 12,700 Oe and consisted of 65.8 wt % Co, 18.3 wt % Sm, and 15.9 wt % Pr. Magnet P-229, a much poorer magnet, had an intrinsic coercive force of only 2,750 Oe and consisted of 66.7 wt % Co, 26.8 wt % Sm, and 6.5 wt % Pr.

Comparison of the two microstructures (Figs. 14 and 15) reveals several differences in microstructure. Magnet P-286 contains more of a gray second phase and somewhat less porosity than magnet P-229. Magnet P-229 also contains larger clear regions devoid of porosity and visible structure, suggesting the presence of large particles in the unsintered powder.

Magnetic Domain Structures

When polarized light is reflected from the surface of a magnetized body, the plane of polarization may be rotated (the Kerr effect). Domains that are magnetized in opposite directions will rotate the polarization in opposite direction, allowing the observation of magnetic domain structures with polarized light.

The two Co-Sm-Pr magnets described above, P-286 and P-229, were studied in polarized light in zero applied field. They were first observed after magnetization in one direction, and then observed at several stages of

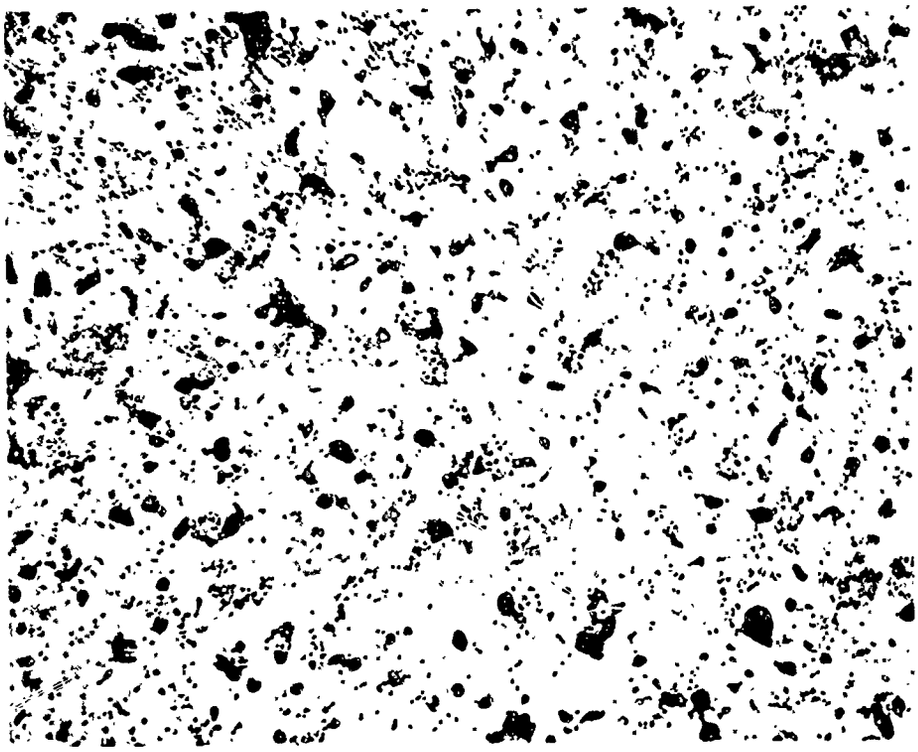

NOT REPRODUCIBLE Fig. 14 Magnet P-286. 750X

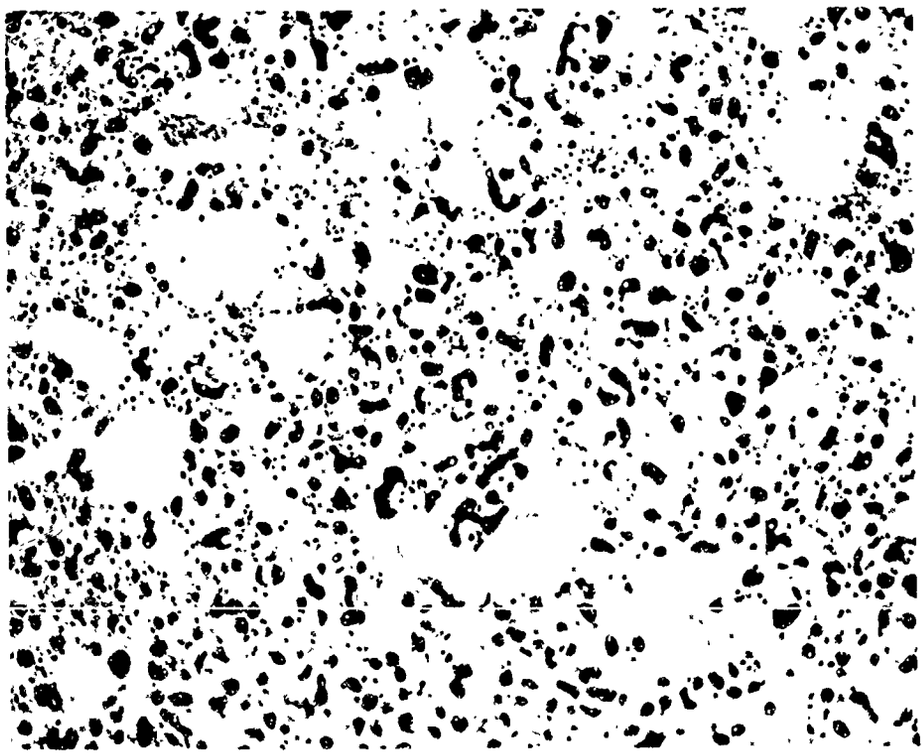

Fig. 15 Magnet P-229. 750X

magnetization reversal after the application of various reverse fields. It was found that the mechanism of magnetization reversal, as revealed by domain observations, was strikingly different for the two magnets.

P-286. In the initial condition, only a small fraction of magnet P-286 showed reversed magnetization (Fig. 16). Although a few large grains showed a mixed domain structure, nearly all the reversed regions appeared to consist of single grains. (The size and position of grains were judged by the distribution of porosity.)

After the application of a reverse field of 11,000 Oe, a larger fraction of the sample was reversed (Fig. 17). Again most of the reversed regions consisted of single grains. Although a few large grains showed domain structure, some grains as large as 40μ in diameter remained unreversed. Thus it is possible for grains of this size to exhibit a high coercive force.

The application of a reverse field of 12,800 Oe, approximately equal to the intrinsic coercive force, reversed approximately half the magnet. However, the reversal was macroscopically nonuniform. Some areas as large as 1 mm^2 were as much as two-thirds reversed, whereas other equally large areas were only one-third reversed. More domain structure was apparent (Fig. 18).

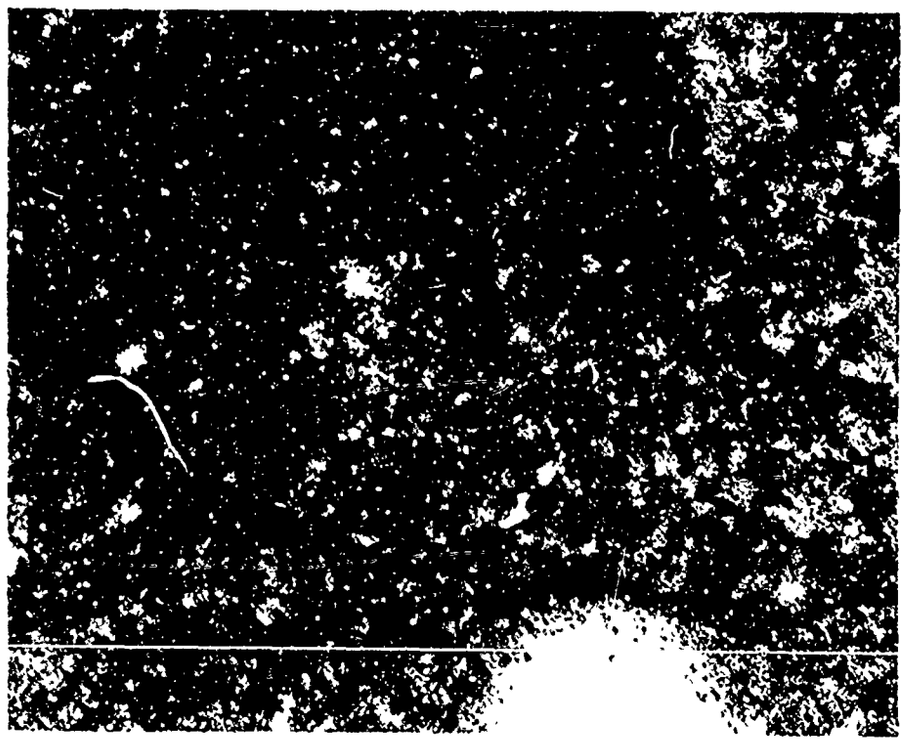

Fig. 16 Magnet P-286. Previously saturated. Polarized light. 500X

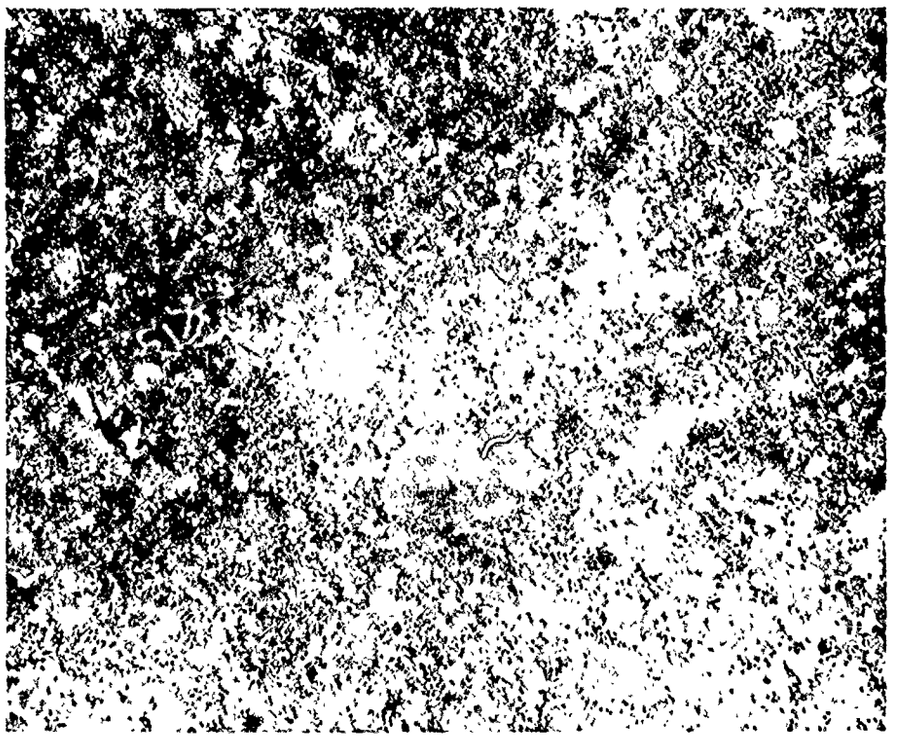

Fig. 17 Magnet P-286. After application of reverse field of 11,000 Oe. Polarized light. 500X

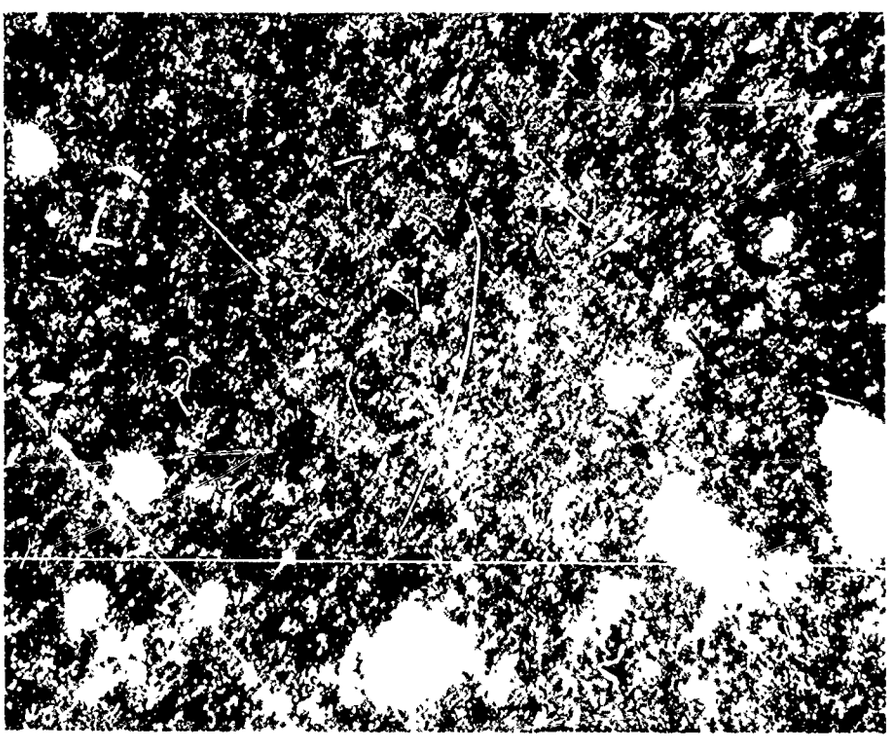

Fig. 18 Magnet P-286. After application of reverse field of 12,800 Oe. Polarized light. 500X

After the application of a reverse field of 17,300 Oe, only a small fraction of the sample remains unreversed (Fig. 19). Much of the unreversed region consists of small completely unreversed grains, but considerable domain structure also exists.

P-229. In direct contrast to P-286, reversal in P-229 takes place almost exclusively through the development of domain structures within grains (Figs. 20, 21, and 22). Few completely reversed grains can be seen.

Thus the magnetization reversal behavior of magnet P-286 much more nearly approaches the ideal of single-domain-particle behavior than does that of magnet P-229.

More work is planned to study the dynamics of domain nucleation and growth in cobalt-rare earth magnets, and to attempt to correlate various observed modes of magnetization reversal with microstructural details such as second-phase particles, porosity, etc.

Co-27 Wt % Sm Magnet. The domain structure of an unmagnetized sintered magnet of Co-27 wt % Sm was observed by polarized light. Regions believed to be Co_5Sm showed a much coarser domain structure than did most

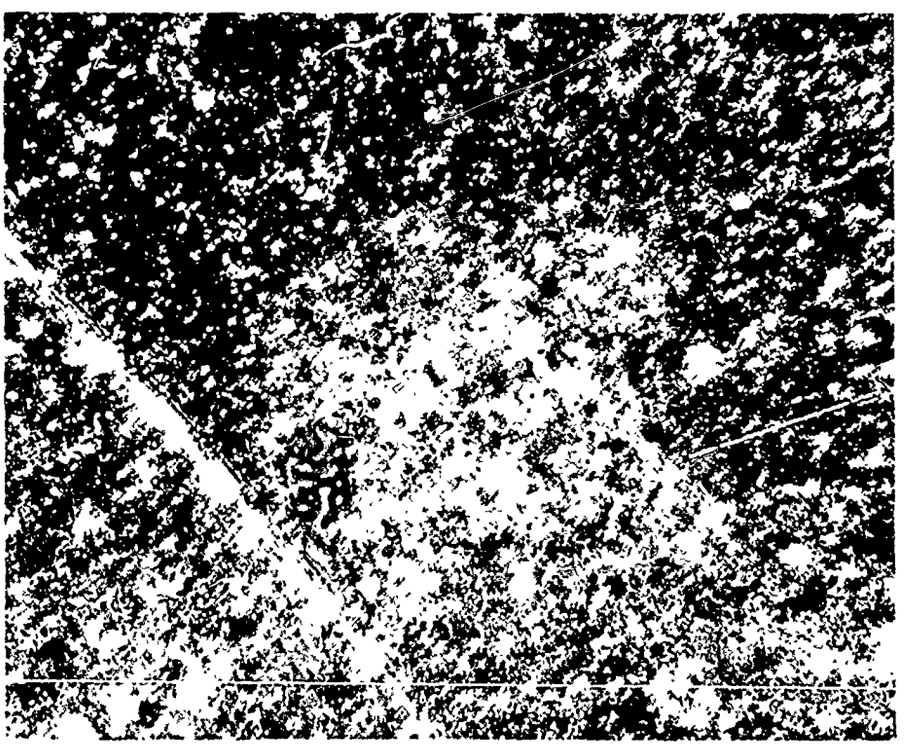

Fig. 19 Magnet P-286. After application of reverse field of 17,300 Oe. Polarized light. 500X

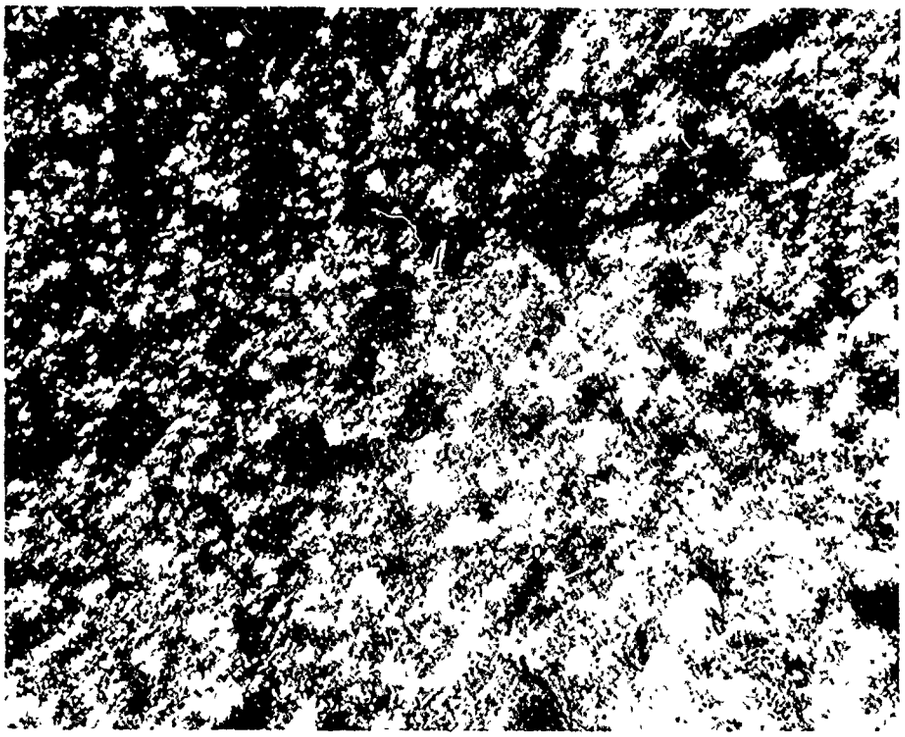

Fig. 20 Magnet P-229. After application of reverse field of 1700 Oe. Polarized light. 500X

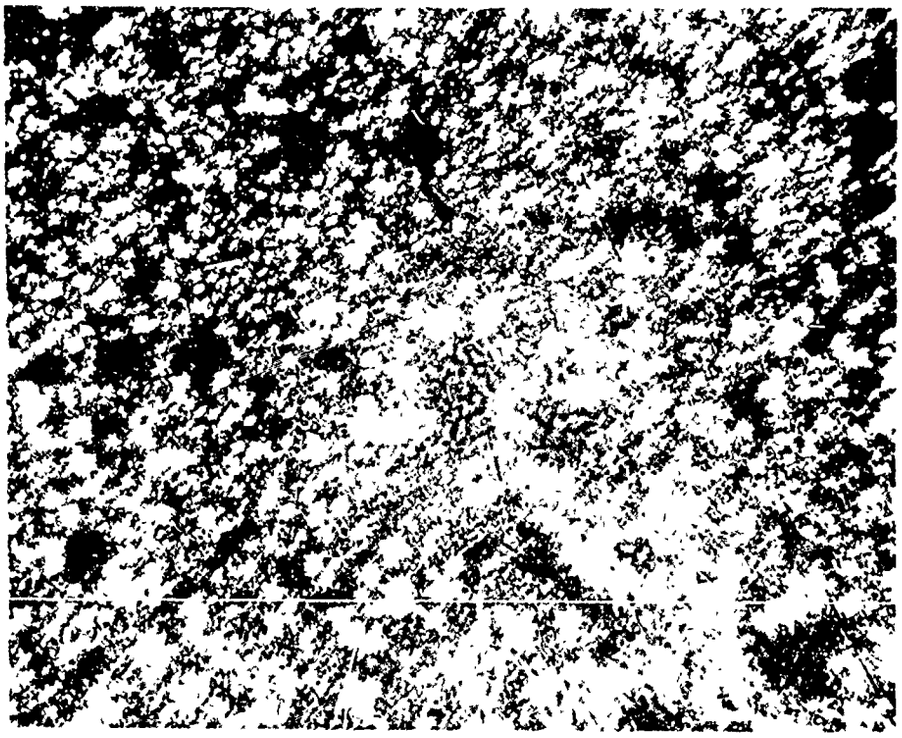

Fig. 21 Magnet P-229. After application of reverse field of 2800 Oe. Polarized light. 500X

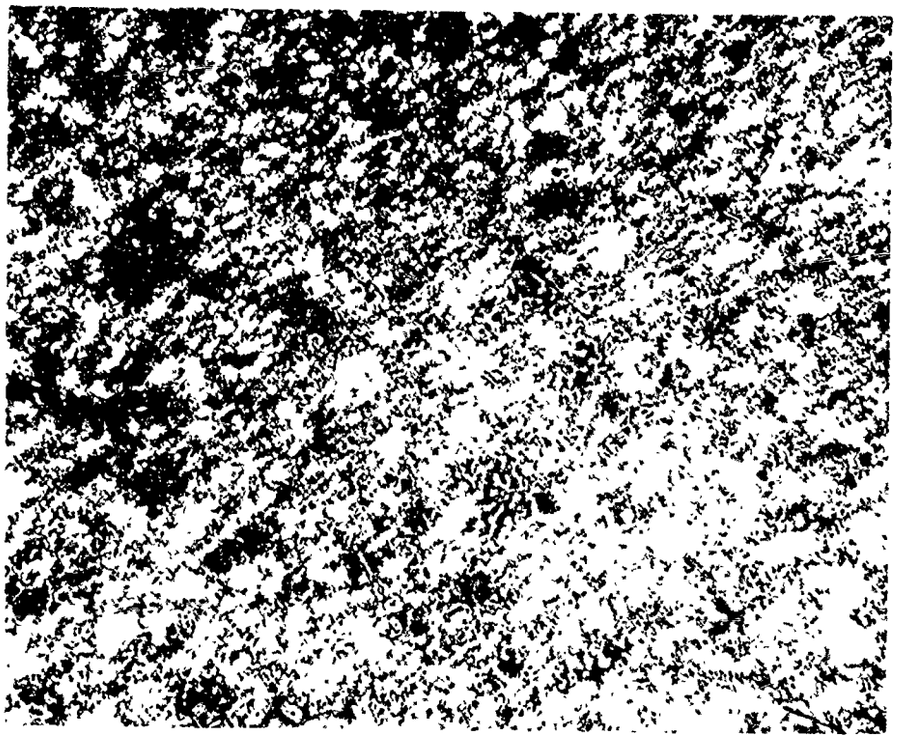

Fig. 22 Magnet P-229. After application of reverse field of 5500 Oe. Polarized light. 500X

of the sample, which is believed to be $Co_{17}Sm_2$ (Fig. 23). This may indicate a significantly lower domain-wall energy in $Co_{17}Sm_2$ than in Co_5Sm, perhaps as a result of a significantly lower crystal anisotropy.

III. INVESTIGATION OF PHASE EQUILIBRIA IN TRANSITION METAL-RARE EARTH SYSTEMS

1. Analysis for Rare Earth Present in the Reduced State by Selective Oxidation (R. E. Cech)

The Co_5-rare earth compounds may be viewed as combinations of a relatively noble or difficult-to-oxidize metal (cobalt) and highly reactive rare earth metals. It should, therefore, be possible to selectively oxidize the rare earth while maintaining the cobalt in a reduced state. If one carries out this selective oxidation of rare earth, the weight gain due to oxygen pickup can be used as a measure of only that portion of the rare earth element in the sample which exists in the reduced state. For example, for samarium (Sm°, At wt = 150.35) oxidized to Sm^{+3} the Sm:O factor would be:

$$\frac{2 \times \text{At wt Sm}}{3 \times \text{At wt Oxygen}} = 6.2646.$$

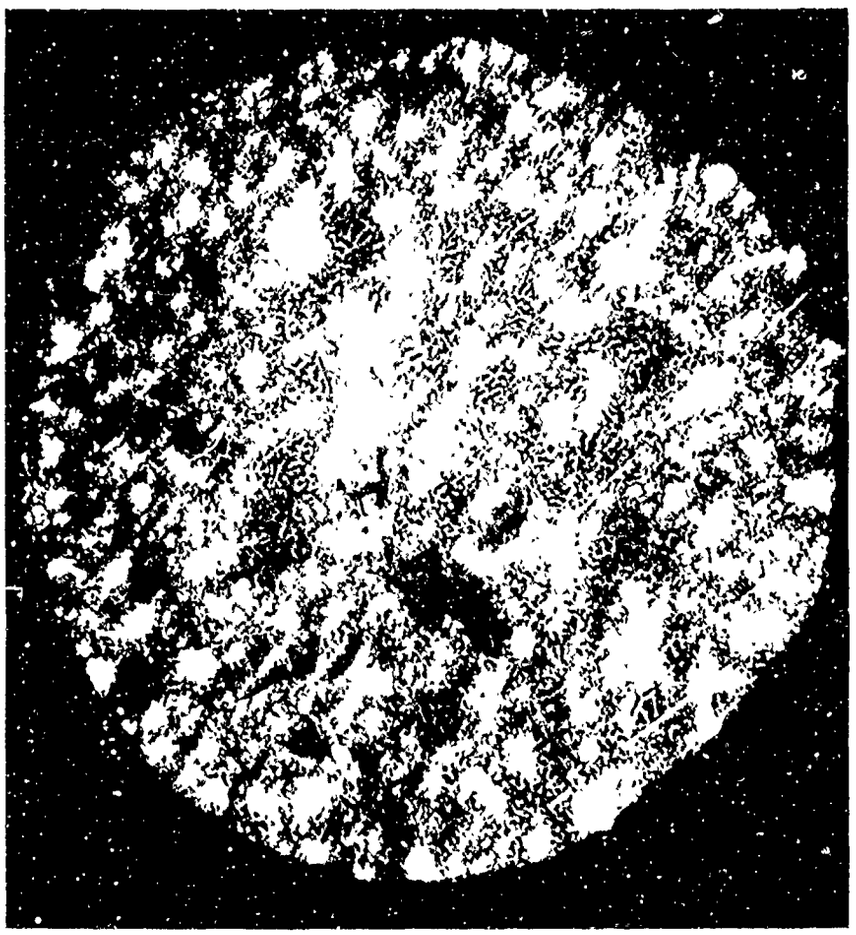

Fig. 23 Unmagnetized sintered magnet of 73% Co and 27% Sm. Polarized light. 500X

From this one could determine percent reduced samarium:

$$\% \text{ Sm} = \frac{\Delta W(\text{from oxygen pickup}) \times 6.2646 \times 100}{\text{Sample wt}}$$

For the elements praseodymium and cerium that have both +3 and +4 oxidation states, it would be necessary to determine empirically the oxidation state of the selectively oxidized rare earth element under a standard set of furnacing conditions.

The atmosphere for carrying out this process could be varied over a wide range of operating conditions.

If one considers the reaction:

$$CoO + H_2 \rightarrow Co + H_2O \quad \Delta F^\circ_{1000^\circ K} = -6,050 \text{ cal.}$$

$$K = \frac{pH_2O}{pH_2} = 21$$

For 1 atm of 750 torr:

$$pH_2O = 716 \text{ torr}$$

$$pH_2 = 34 \text{ torr.}$$

One could obtain wet hydrogen by passing H_2 through water at any temperature up to 98.4°C and still maintain cobalt in the reduced state while oxidizing the rare earth element.

As an alternative to this procedure one could oxidize the sample completely and then selectively reduce the cobalt using hydrogen of any desired dew point. If one considers that a hydrogen dew point of -90°C is about the dryest gas that one would normally encounter without taking elaborate steps to dry the gas:

$$\frac{pH_2O}{pH_2} = 10^{-7} \text{ for } -90^\circ C \text{ dew point } H_2$$

For the reaction:

$$1/3\ Sm_2O_3 + H_2 \rightarrow 2/3\ Sm + H_2O \quad \Delta F^\circ_{1000^\circ K} = +76,200 \text{ cal.}$$

$$\log_{10}K = -16.66$$

$$K = \frac{pH_2O}{pH_2} = 10^{-16.66}.$$

Thus, dry hydrogen cannot reduce Sm_2O_3.

A simple procedure may be carried out to selectively oxidize the rare earth element with wet hydrogen if one includes a small rubber stoppered "U" tube at the gas inlet point of the reaction tube. The system containing the Co_5-rare earth powder specimen can be flushed with N_2, then raised to temperature under dry H_2. A small amount of water can then be injected into the "U" tube using a hypodermic syringe. After all the water has been

evaporated into the flowing H_2 stream, the system then reverts to dry H_2 needed for cooling the system to room temperature.

A series of oxidation and reduction experiments was performed using mixed sample 3943B13-16 (2.6943 grams). All heat treatments were for 1 hour in designated atmospheres:

1. Dry hydrogen, nominally -60°C dew point.
2. Wet hydrogen, +25°C dew point.
3. Air.

Specimens treated in wet hydrogen were given an additional 10 minutes at temperature in dry hydrogen before cooling.

It was noted that selectively oxidized Co_5Sm or reduced CoO would pick up weight on exposure to the atmosphere, presumably because of adsorption of oxygen from the atmosphere. This would cause a variation in ΔW leading to an apparent change in Sm° (reduced samarium) content. The following results illustrate the point:

	Wt % Sm°
Specimen after 2 hours in wet H_2, promptly weighed in air----	32.99
Specimen stirred in air using clean S.S. spatula----------	33.18
Specimen aged in room air at room temperature 1 hour-------	33.43

In order to minimize errors due to this effect, and recognizing that the initial powder is coated with adsorbed oxygen, all samples were stirred in air and weighed promptly.

The following results were obtained on sample 3943B13-16:

	Wt % Sm°
1 hour 800°C, wet H_2	32.95
+1 hour 800°C, wet H_2	33.18
+1 hour 800°C, wet H_2	33.11
+1 hour 800°C, air (complete oxidation)	
+1 hour 800°C, dry H_2	33.97
+1 hour 800°C, dry H_2	33.69

The true Sm° content must lie somewhere between 33.18% and 33.69%. One can simply presume that it lies midway between the selective oxidation and selective reduction figure. The true Sm° content would then be 33.44 wt %. Note that the same figure is obtained by averaging the results of the first hour of oxidation and reduction as is found by averaging the second hour of each.

The following procedure is suggested for determination of Sm°:

1. Selective oxidation in wet H_2 1 hour at 800°C.
2. Determine wt of stirred sample.
3. Oxidize completely in air.
4. Reduce for 1 hour at 800°C in dry H_2.
5. Determine wt of stirred sample.
6. Average ΔW and calculate the percent of Sm° from the stoichiometry factor.

Also, the "aged one hour at R. T." should be checked to see if the agreement here is fortuitous.

2. Oxidation Studies and Analytical Techniques (J. G. Smeggil)

A freshly cleaved surface of a sample of Sm-Co alloy containing nominally 66 wt % Co and 34 wt % Sm was obtained by fracturing a fragment of the sample. This surface was photographed at 28X daily for a week, using an unchanged configuration of camera, lights, and sample surface, to determine if any surface oxidation could be visually observed. While it is difficult to make definitive comments on this experiment, there was a noticeable difference between the photographs taken on the first and last days. The surface seemed to be becoming fuzzy, as though it were less smooth. In order to document any changes more quantitatively, a similar study will be undertaken using the scanning electron microscope.

A finished Co-Sm magnet was cut lengthwise and has been submitted for analysis by electron probe techniques to determine if there is any macroscopic variation of the concentration of Co Sm, O, and N along the length and width of the magnet.

Powder samples from the powder storage experiment described by Benz et al.[14] were obtained and submitted for x-ray diffraction, vacuum fusion, and emission spectroscopy analyses. The sample numbers, sample history, and colors are:

Sample no.	Storage test no.	Storage conditions (1 month)	Color
1	4	Air - open - 150°C	Blue
2	1	Air - open	Grey
3	3	Air - closed - wet	Brown
4	2	Air - closed - dry	Grey

The x-ray diffraction analyses indicated that all four samples contained two phases, Co_5Sm and Co_2Sm. Minor amounts of Co_2Sm were detected in samples from storage tests 4 and 2 while storage tests 3 and 1 contained larger amounts of this phase. Lattice parameters for the Co_5Sm phase present are:

Sample no.	a	c
1	5.005 A	3.971 A
2	5.000	3.973
3	4.998	3.974
4	4.999	3.972

The error in these values is ± 0.003 A. Therefore all these samples have the same lattice parameter within the error reported.

The emission spectroscopy and vacuum fusion analyses for these samples are as follows (all figures in ppm):

Sample no.	B	Na	Si	Al	Ca	Ti	Fe
1	10	30	10	800	<10	<10	200
2	<10	<30	10	800	<10	<10	200
3	<10	<30	10	800	<10	<10	200
4	<10	100	10	900	<10	<10	300

Ni	Cu	Sn	Mn	Cr	O	N	H
3000	<10	<10	<10	<10	42,300 ± 500	174 ± 13	84 ± 7
3000	<10	<10	<10	<10	4,770 ± 350	171 ± 13	101 ± 9
3000	<10	<10	<10	<10	10,500 ± 400	187 ± 14	215 ± 20
3000	<10	<10	<10	<10	4,670 ± 350	167 ± 13	88 ± 7

Samples 1 through 4 and a small piece of finished Co_5Sm magnet, sample no. T-5-3-2, made from powder stored wet, will be examined by high-temperature x-ray techniques to determine, in the case of the powders, the effect high temperatures might have on forming an ordered oxide phase, and, in the case of the finished magnet, if there are any order-disorder transitions occurring in this system as a function of temperature.

A sample of the same finished magnet has been submitted for vacuum fusion analysis to determine if the final sintering process significantly changes the amount of O and N present as compared with that found in the powder.

New analytical techniques are being sought with respect to Sm analyses. Emphasis is being placed on finding a wet technique for determining Sm with an accuracy of $\sim \pm 0.1$ wt % for analyzing magnets showing exceptional properties, and secondly finding an instrumental technique, possibly x-ray fluorescence spectroscopy, with an accuracy of ± 0.1 wt % Sm. This second technique would find its greatest use as a quality control tool in the fabrication of these magnets.

IV. IDENTIFICATION AND INVESTIGATION OF NEW MATERIALS

1. Alloy Development (D. L. Martin)

The development of cobalt-rare earth alloy permanent magnets with energy product values approaching 30 mGOe appears to be a realistic goal based on what has already been achieved by numerous investigators and the theoretical potential of the cobalt-rare earth alloys. However, to achieve 30 mGOe will require careful optimization of a large number of variables such as composition, particle alignment, and density.

Past work on the permanent magnet, cobalt-rare earth alloys has centered on the Co-Sm system[9-16]. In that system, alloys with energy product values in the range 15-20 mGOe have been reported generally[10-15]. Somewhat higher energy product values up to 23 mGOe have been attained by replacing some of the samarium with praseodymium[17].

The theoretical limit of the energy product is $(4\pi J_S)^2/_4$ where $4\pi J_S$ is the saturation magnetization. To attain this limiting value requires perfect packing and alignment of the magnetic particles as well as a high degree of resistance to demagnetization. $(BH)_{max}$ values as high as 75-85% of the $(4\pi J_S)^2/_4$ value have been reported by Martin and Benz[17] for a variety of cobalt-rare earth permanent magnet alloys. If one assumes that 80% of the limit is generally achievable, then to have a $(BH)_{max}$ of 25 mGOe would require a saturation value of about 11,000 gauss and a 30 mGOe magnet would require over a 12,000 gauss saturation value.

The saturation values for some Co_5R* alloys are listed in Table I. The Co-Pr and Co-Nd systems with $4\pi J_S$ values over 12,000 gauss are the most attractive of the binary Co_5R systems. Unfortunately, the c axis is not a direction of easy magnetization in the Co_5Nd crystal[18] and the magneto-crystalline anisotropy constant is much lower than for the other Co_5R phases[10, 19]. Therefore, it is unlikely that the binary Co-Nd alloys will yield permanent magnets with energy products above 25 mGOe. On the other hand Nd additions to the other Co_5R alloys may increase the saturation without changing the uniaxial anisotropy. Small additions of neodymium to Co_5Pr have

---

*"R" refers to any of the rare earth metals.

TABLE I

Saturation Magnetization Values for Some Co_5R Alloys

Alloy	$4\pi J_S$	Reference
Co_5Nd	12280	2
Co_5Pr	12030	2
$Co_5Pr_{.05}Sm_{0.5}$	12050	9
Co_5Y	10600	2
Co_5Sm	9600*	2
Co_5La	9090	2
Co_5Ce	7700	2

*The author has measured values as high as 10,200 gauss at 100 kG.

been reported to increase the saturation 12% above the value for the binary Co_5Pr[20].

The addition of praseodymium to Co_5Sm has been shown to increase the saturation without impairing the magnetic properties[17]. As mentioned the Co-Pr-Sm alloys have $(BH)_{max}$ values higher than have been obtained in the binary Co-Sm alloys. The highest reported value is 2[illegible] mGOe[17].

Saturation is only one of four important parameters needed to yield a high energy magnet. The other three are: the packing fraction, the alignment and the demagnetization resistance. Before discussing these parameters and showing how they relate to the B:H curve it is worthwhile to describe how we plan to process the magnets.

The Co_5R alloy in the as cast condition is a poor magnet. To make a high energy magnet it is necessary to grind the cast metal into fine powder, align the particles in a magnetic field, and densify by pressing and/or sintering. A particular process, which has been successfully used to make high-energy product cobalt-samarium magnets[13] and ternary cobalt-rare earth alloy magnets[17] will be used in this study. It has been called liquid phase sintering and involves the blending of a base metal, Co_5R phase with a sintering aid, an alloy richer in rare earth than the base metal, aligning the powder in a magnetic field, isostatic pressing, and sintering. This liquid phase sintering process has worked well for making magnets in the Co-Sm, Co-Pr, Co-Pr-Sm, Co-La-Sm, Co-Ce-Sm, Co-MM-Sm systems[17] and in the Co-Pr-Nd-Sm system[20].

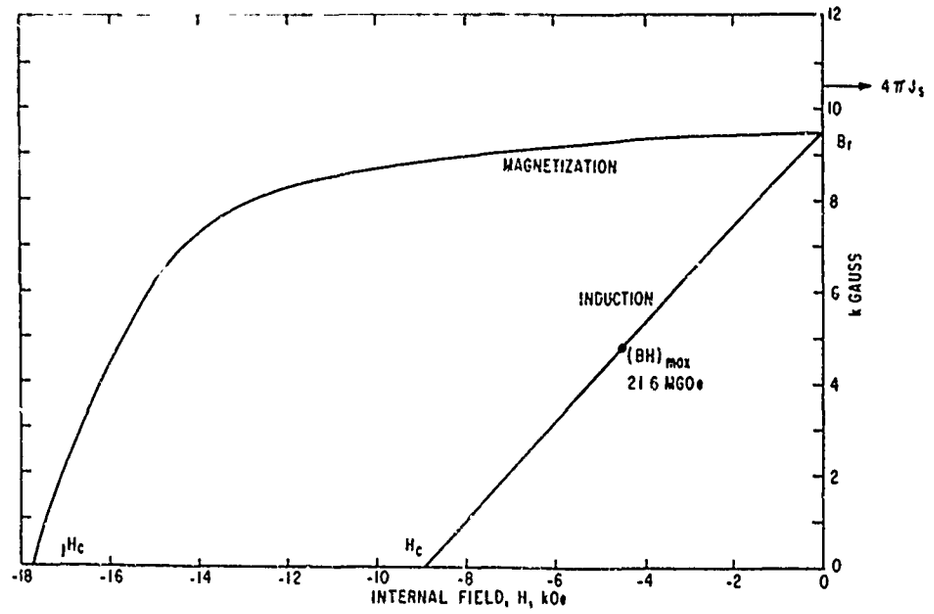

Fig. 24 Demagnetization curves for a sintered and 900°C aged sample of 63.3% Co, 20.2% Sm, 15.9% Pr alloy (after Martin and Benz[23]).

The cobalt rare earth permanent magnets often have a linear induction demagnetization curve as shown in Fig. 24 for a Co-Sm-Pr alloy magnet. The theoretical limit for this magnet based on the saturation value of 10.5 K Gauss is 27.5 mGOe. To attain the theoretical limit requires perfect alignment and packing of the magnetic particles. For this sample the alignment and packing were 0.95*. The residual induction B_r, is equal to $PA(4\pi J_s)$, and for this sample is about 0.9 times the saturation value. If the magnet has a high degree of resistance to demagnetization so that $_jH_c \gg B_r$, then $H_c \approx B_r$. For the sample in Fig. 24, $H_c = 0.93\ B_r$. For a linear B:H curve, the $(BH)_{max}$ value is $(B_r \cdot H_c)/4$. Since $B_r = PA(4\pi J_s)$ and $H_c \approx B_r$, one can write

$$(BH)_{max} = \theta P^2 A^2 \frac{4\pi J_s}{4} \qquad (1)$$

The factor, θ, is introduced to account for the fact that H_c does not usually equal B_r. That is $\theta = H_c/B_r$. This relation clearly shows the importance of having a high degree of alignment and a high packing fraction of the magnetic particles. The combination term $\theta P^2 A^2$ has been found to be in the range

---

*Alignment, A, is defined as the ratio of $B_r/4\pi J_{100}$. That is the ratio of magnetization at a peak field of 100 kOe to that at zero field. The packing fraction, P, is the ratio of the density of the sample to that of the alloy.

0.75 to 0.85 for many of the systems studied[17]. That is, the energy product will be 75 to 85% of the theoretical limit determined from the saturation value.

Experimental program

The initial alloy systems selected for study in this program are Co-Pr, Co-Pr-Sm, Co-Nd-Sm, and Co-Pr-Nd-Sm. In this report results for some alloys in the Co-Nd-Sm and Co-Pr-Nd-Sm systems will be given.

Cylindrical test bars, 0.3 inch diameter by 1 inch long, for magnetic measurements were made from powder by the same general procedure described in previous reports[13, 14, 17]. The test bars were magnetized at 60 kOe before measurement. The magnetization at 60 kOe and the demagnetization curve data were measured by withdrawing the sample from a search coil in a constant magnetic field as has been described in previous reports[13, 17, 21].

A $Co_5Nd_{0.5}Sm_{0.5}$ base metal alloy was mixed with a 60 w/o Sm- 40 w/o Co sintering additive to make the Co-Nd-Sm series, and mixed with a 30 w/o Pr-30 w/o Sm - 40 w/o Co sintering additive to make the Co-Nd-Pr-Sm series. The blend compositions were varied from 62 to 63.5 w/o Co since past experience has shown this to be the best range for optimum properties[13,17]. The results are tabulated in Table II.

Test data are given for the "as pressed" condition. This is after alignment and hydrostatically pressing at 200K psi. Note that the alignment factor and coercive force as well as the packing fraction increase significantly with sintering. As a result there is a marked improvement in the demagnetization properties. This is shown in Fig. 25 for one of the samples. The high temperature aging treatment gives an additional increase to the coercive force. This treatment was previously found to be effective in improving the demagnetizing resistance of Co-MM-Sm alloys[22] as well as Co-Sm, Co-Pr, Sm, Co-La-Sm, Co-Ce-Sm alloys[23]. This study shows that it is also an effective method for improving the coercive force of some of the Co-Nd-Sm and Co-Nd-Pr-Sm alloys.

The magnetic data are plotted in Figs. 26 and 27 versus the cobalt content of the alloys. The saturation values of the Co-Nd-Sm alloys are no higher than has been observed for Co-Sm alloys while the coercive force values are lower[14, 15].

The results for the Co-Nd-Pr-Sm series are plotted in Fig. 28. The saturation values are slightly higher than would be expected for the binary Co-Sm alloys; however, the coercive force values are lower. It is possible that with additional study one might find a thermal treatment which will increase the coercive force significantly; however, even with considerable improvement these alloys will not exceed the 25 mGOe goal for $(BH)_{max}$. These results do show that Nd and Pr combined are more effective than Nd

Table II Summary of Data for Some Co-Nd-Sm and Co-Nd-Pr-Sm Alloys

Alloy No.	Composition Co	Sm	Nd	Pr	Treatment*	$4\pi J_{60}$ kG	$4\pi J_s$ kG	B_r kG	H_e kOe	$_JH_C$ kOe	$(BH)_{max}$ MGOe	Theor. Limit	Density g/cm^3	Packing Fraction	Alignment
2	62.0	24.6	13.4		As pressed	7.4	9.1	6.7	1.6	1.8	5.0	24	6.88	.81	.92
					+ 1h. 1100°C	8.2	9.1	7.8	3.4	4.1	10.0	48	7.62	.90	.95
					+ 1h. 1110°C, 1 1/2h. 900°C	8.4	9.3	8.0	5.0	8.3	14.0	65	7.72	.91	.94
3	62.5	23.7	13.8		As pressed	7.2	9.0	6.1	1.5	1.7	4.0	19	6.85	.81	.88
					+ 1h. 1100°C	8.2	9.1	7.5	3.4	4.3	10.5	50	7.63	.90	.92
					+ 1h. 1110°C, 1 1/2h. 900°C	8.5	9.1	7.9	5.2	10.0	14.0	68	7.93	.93	.93
4	63.0	23.0	14.0		As pressed	7.5	9.4	6.8	1.6	1.7	5.0	22	6.81	.80	.91
					+ 1h. 1100°C	8.6	9.6	8.1	2.9	3.1	11.0	48	7.64	.90	.95
					+ 1h. 1110°C, 1 1/2h. 900°C	9.1	9.7	8.6	5.0	6.8	16.0	68	7.95	.93	.95
5	63.5	22.1	14.4		As pressed	7.4	9.2	6.3	1.6	1.7	4.5	21	6.82	.80	.87
					+ 1h. 1100°C	8.5	9.5	7.9	2.8	5.3	12.0	54	7.64	.90	.93
					+ 1h. 1110°C, 1 1/2h. 900°C	9.0	9.6	8.4	5.9	8.0	17.0	74	7.93	.93	.94
6	62.0	19.3	13.4	5.3	As Pressed	7.3	9.2	6.6	1.5	1.7	4.5	21	6.79	.80	.92
					+ 1h. 1100°C	9.0	9.9	8.6	5.2	6.5	16.0	66	7.76	.91	.95
					+ 1h. 1110°C, 1 1/2h. 900°C	9.4	10.0	9.0	5.4	8.5	15.0	60	7.99	.94	.96
7	62.5	19.0	13.8	4.7	As pressed	7.5	9.3	6.7	1.6	1.7	5.0	23	6.82	.80	.90
					+ 1h. 1100°C	9.1	10.0	8.7	5.0	6.8	16.5	67	7.72	.91	.96
					+ 1h. 1110°C, 1 1/2h. 900°C	9.5	10.1	9.1	4.0	5.5	13.0	51	7.97	.94	.96
8	63.0	18.8	14.0	4.2	As pressed	7.6	9.6	7.0	1.6	1.7	5.0	22	6.73	.79	.93
					+ 1h. 1100°C	9.3	10.3	9.0	3.0	3.5	12.5	47	7.68	.90	.96
					+ 1h. 1110°C, 1 1/2h. 900°C	9.8	10.5	9.5	1.6	1.8	6.0	22	7.94	.93	.97
9	63.5	18.5	14.4	3.6	As pressed	7.7	9.7	6.9	1.6	1.7	5.0	21	6.77	.80	.91
					+1 h. 1100°C	9.5	10.5	9.0	3.0	3.3	13.0	47	7.68	.90	.95
					+1 h. 1110°C, 1 1/2h. 900°C	10.0	10.6	9.7	5.2	6.1	20.0	71	8.06	.95	.96

* The heat treatments were done in purified argon

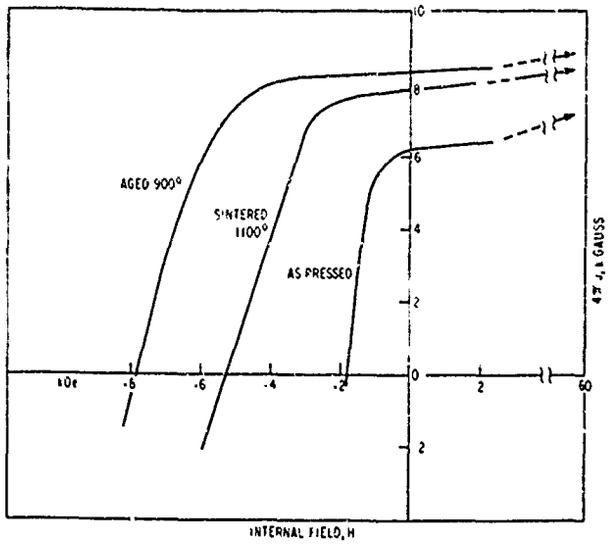

Fig. 25 Effect of sintering and 900°C aging on the demagnetization curve for a Co-Sm-Nd alloy (No. 5 in Table II).

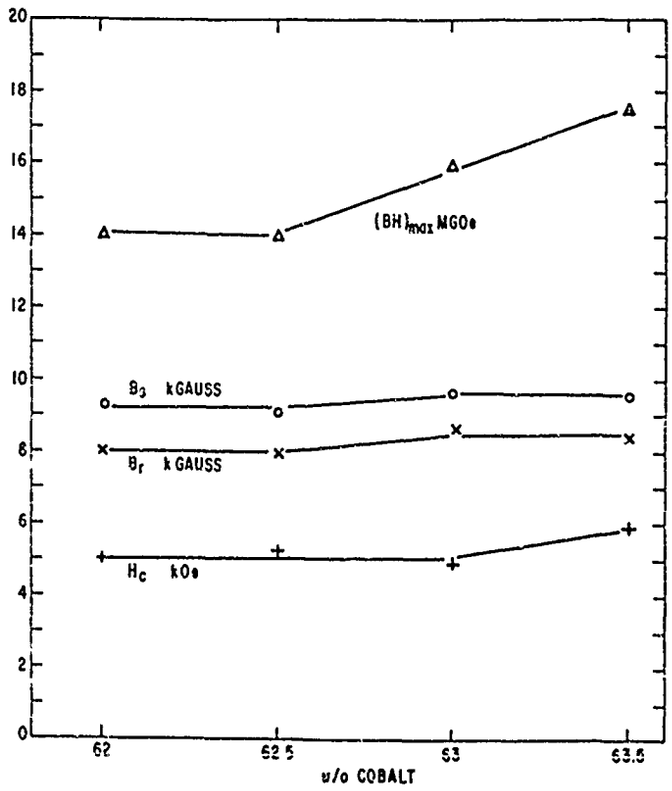

Fig. 26 Magnetic properties of a series of Co-Nd-Sm alloys sintered 1 hour at 1110°C and aged 1 1/2 hour at 900°C.

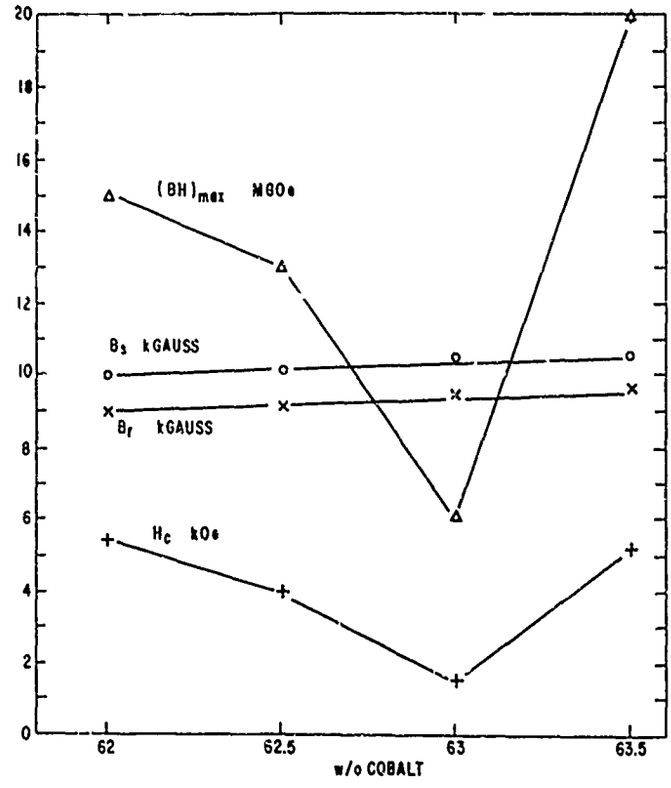

Fig. 27 Magnetic properties of a series of Co-Nd-Pr-Sm alloys sintered 1 hour at 1110°C and aged 1 1/2 hour at 900°C.

alone in increasing the saturation. The results obtained in this study are somewhat higher than those reported by Tsui, Strnat, and Harmer[20].

The change of properties with composition is quite different for these two series than for the Co-Pr-Sm system alloys. Note the difference between Figs. 26 and 27 and Fig. 28. This is a puzzling difference which cannot be explained without more study.

There is need for additional work on both of these alloy systems, but not necessarily on these particular alloys since the saturation values are lower than is needed to attain a $(BH)_{max}$ greater than 25 mGOe. Future work will be directed to increasing the Pr, Nd and Nd+Pr content in these and the other systems being studied.

2. Magnetic Behavior of Co_7R_2 Compounds (J. J. Becker)

The successful preparation of high-performance cobalt-rare earth permanent magnets seems to require that the final overall composition be on the rare earth-rich side of the Co_5R composition, presumably because of the

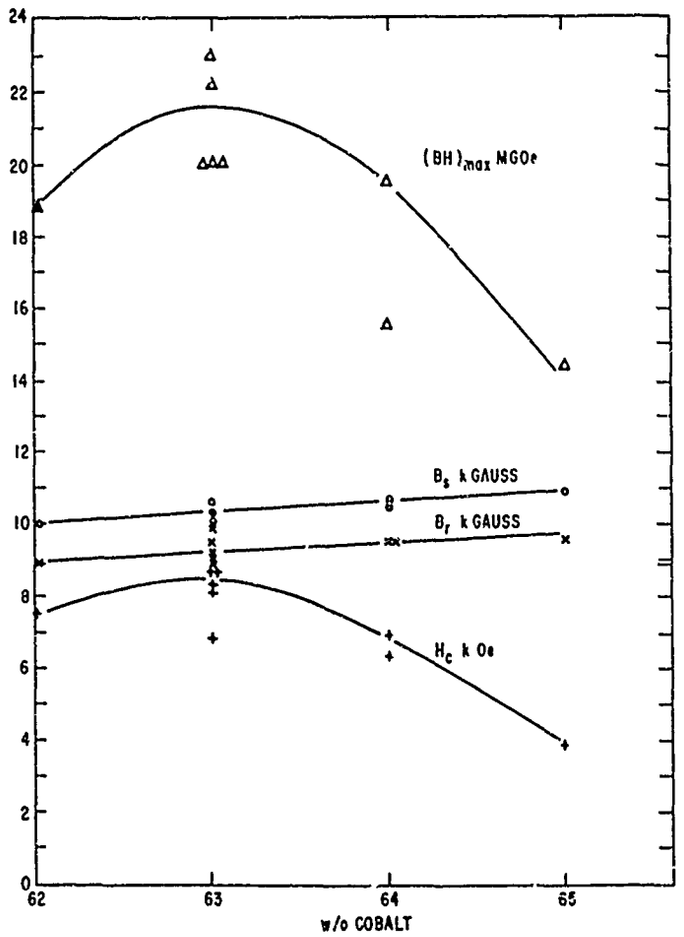

Fig. 28 Magnetic properties of a series of sintered Co-Pr-Sm alloys (after Martin and Benz[17]).

requirements for successful liquid-phase sintering. Thus it seemed appropriate to examine the magnetic properties of some Co_7R_2 compounds in more detail. Several alloys were prepared with the following nominal compositions:

Co 57.84% Sm 42.16%
Co 69.88% Y 30.12%
Co 59.55% Ce 40.45%
Co 58.85% Nd 41.15%
Co 59.76% La 40.24%
Co 59.41% Pr 40.59%

These correspond to Co_7R_2 in each instance. This compound may not necessarily exist in every case. Metallography and x-ray diffraction studies have not yet been done. These materials were simply ground to -325 mesh powder and their coercive force measured. The results were as follows:

Rare Earth	Intrinsic Coercive Force
Sm	4300 Oe (H_m = 21 kOe), 5200 Oe (H_m = 30 kOe)
Y	360 Oe (H_m = 21 kOe)
Pr	810 Oe (H_m = 21 kOe)
Ce	1210 Oe (H_m = 21 kOe)
Nd	475 Oe (H_m = 21 kOe)
La	320 Oe (H_m = 21 kOe)

The pronounced difference between the Sm compound and all the others is entirely analogous to the behavior of the 5 - 1 series and raises the same question: Why is the Sm compound so different?

REFERENCES

1. J.J. Becker, R.E. Cech, J.S. Kasper, and J.S. Kouvel, Air Force Materials Laboratory Summary Technical Report AFML-TR-68-54, April 1968.

2. J.J. Becker, IEEE Trans. on Magnetics MAG-5, 211 (1969).

3. H. Zijlstra, IEEE Trans. on Magnetics MAG-6, 179 (1970).

4. H. Zijlstra, J. Appl. Phys. 41, 4881 (1970).

5. C.D. Graham, Jr., J.J. Becker, and I.S. Jacobs, Air Force Materials Laboratory Final Report AFML TR-65-253, September 1965.

6. H. Zijlstra, Rev. Sci. Inst. 41, 1241 (1970).

7. Y.S. Shur and V.I. Khrabov, Soviet Physics J.E.T.P. 30, 1027 (1970).

8. C. Kooy and U. Enz, Philips Res. Repts. 15, 7 (1960).

9. K. Strnat, G. Hoffer, J.C. Olson, W. Ostertag and J.J. Becker, J. Appl. Phys., 38, 1967 1001.

10. W. Velge and K. Buschow, J. Appl. Phys., 39, 1968, 1717.

11. F. Westendorp and K. Buschow, Solid State Commun., 7, 1969, 639.

12. D. Das,IEEE Trans. Magnetics, MAG-5, 1969, 214.

13. M. Benz and D. L. Martin, Appl. Phys. Letters, 17, 1970, 176.

14. M. G. Benz, et al., Interim Tech. Report IR-612-9A(3), Aug. 1970, Air Force Materials Laboratory, Dayton, Ohio.

15. D. Das, et al., Interim Report IR-612-9B(3), December, 1970. Air Force Materials Laboratory, Dayton, Ohio.

16. R. E. Cech, J. Appl. Physics, 41, 1970.

17. D. L. Martin and M. G. Benz, International Conference on Magnetism, Sept. 1970, Grenoble, France; also, Cobalt, March 1971.

18. R. Lemaire, Cobalt 32, 1966, 132.

19. K. J. Strnat, IEEE Trans. Magnetics, MAG-6, 182, (1970).

20. J. Y. B. Tsui, K. J. Strnat and R. S. Harmer, 16th Annual Conference on Magnetism and Magnetic Materials, Miami, November 1970. To be published in J. Appl. Physics, March 1971.

21. M. G. Benz and D. L. Martin, "Measurement of Magnetic Properties of Cobalt-Rare Earth Permanent Magnets", IEEE Conference on Electron Device Techniques, Sept. 1970. To be published in IEEE Trans. Magnets some time in 1971.

22. M. G. Benz and D. L. Martin, 16th Annual Conference on Magnetism and Magnetic Materials, Miami, Nov. 1970. To be published in J. Applied Phys., March 1971.

23. D. L. Martin and M. G. Benz, unpublished work.